Circulation

ORIGINAL RESEARCH ARTICLE

Targeting NPM1 Epigenetically Promotes Postinfarction Cardiac Repair by Reprogramming Reparative Macrophage Metabolism

Sheng Zhang, PhD*; Yunkai Zhang, PhD*; Xuewen Duan, MS; Bo Wang, PhD; Zhenzhen Zhan, MD, PhD

BACKGROUND: Reparative macrophages play a crucial role in limiting excessive fibrosis and promoting cardiac repair after myocardial infarction (MI), highlighting the significance of enhancing their reparative phenotype for wound healing. Metabolic adaptation orchestrates the phenotypic transition of macrophages; however, the precise mechanisms governing metabolic reprogramming of cardiac reparative macrophages remain poorly understood. In this study, we investigated the role of NPM1 (nucleophosmin 1) in the metabolic and phenotypic shift of cardiac macrophages in the context of MI and explored the therapeutic effect of targeting NPM1 for ischemic tissue repair.

METHODS: Peripheral blood mononuclear cells were obtained from healthy individuals and patients with MI to explore NPM1 expression and its correlation with prognostic indicators. Through RNA sequencing, metabolite profiling, histology, and phenotype analyses, we investigated the role of NPM1 in postinfarct cardiac repair using macrophage-specific NPM1 knockout mice. Epigenetic experiments were conducted to study the mechanisms underlying metabolic reprogramming and phenotype transition of NPM1-deficient cardiac macrophages. The therapeutic efficacy of antisense oligonucleotide and inhibitor targeting NPM1 was then assessed in wild-type mice with MI.

RESULTS: NPM1 expression was upregulated in the peripheral blood mononuclear cells from patients with MI that closely correlated with adverse prognostic indicators of MI. Macrophage-specific NPM1 deletion reduced infarct size, promoted angiogenesis, and suppressed tissue fibrosis, in turn improving cardiac function and protecting against adverse cardiac remodeling after MI. Furthermore, NPM1 deficiency boosted the reparative function of cardiac macrophages by shifting macrophage metabolism from the inflammatory glycolytic system to oxygen-driven mitochondrial energy production. The oligomeric NPM1 recruited histone demethylase KDM5b to the promoter of *Tsc1* (*TSC complex subunit 1*), the mTOR (mechanistic target of rapamycin kinase) complex inhibitor, reduced histone H3K4me3 modification, and inhibited TSC1 expression, which then facilitated mTOR-related inflammatory glycolysis and antagonized the reparative function of cardiac macrophages. The in vivo administration of antisense oligonucleotide targeting NPM1 or oligomerization inhibitor NSC348884 substantially ameliorated tissue injury and enhanced cardiac recovery in mice after MI.

CONCLUSIONS: Our findings uncover the key role of epigenetic factor NPM1 in impeding postinfarction cardiac repair by remodeling metabolism pattern and impairing the reparative function of cardiac macrophages. NPM1 may serve as a promising prognostic biomarker and a valuable therapeutic target for heart failure after MI.

Key Words: epigenesis, genetic ■ macrophages ■ metabolic reprogramming ■ myocardial infarction ■ nucleophosmin ■ oligonucleotides, antisense

Correspondence to: Zhenzhen Zhan, MD, PhD. Shanghai Institute of Transplantation, Renji Hospital, Shanghai Jiao Tong University School of Medicine, 160 Pujian Rd, Shanghai 200127, China. Email zhanzz@tongji.edu.cn
*S. Zhang and Y. Zhang contributed equally.
Supplemental Material is available at https://www.ahajournals.org/doi/suppl/10.1161/CIRCULATIONAHA.123.065506.
For Sources of Funding and Disclosures, see page 2000.

Circulation is available at www.ahajournals.org/journal/circ

Clinical Perspective

What Is New?

- NPM1 (nucleophosmin 1) deficiency in macrophages ameliorates myocardial ischemic injury, improves cardiac function, and promotes tissue repair after myocardial infarction by shifting cardiac macrophages toward the oxidative phosphorylation metabolism and reparative phenotype.
- The epigenetic inhibition of TSC1 (TSC complex subunit 1) mediated by the interaction of NPM1 and histone demethylase KDM5b enhances the mechanistic target of rapamycin kinase pathway activation and boosts glycolytic metabolism, thereby maintaining the inflammatory phenotype of cardiac macrophages and impeding ischemic tissue repair.
- The in vivo therapeutic treatment targeting NPM1 through antisense oligonucleotide or oligomerization inhibitor both markedly attenuate adverse ventricular remodeling and improve cardiac repair in mice after myocardial infarction.

What Are the Clinical Implications?

- The upregulated NPM1 in peripheral blood mononuclear cells has strong correlations with aggravated cardiac injury, cardiac dysfunction, and heart failure after myocardial infarction stress, implying that NPM1 serves as a promising adverse prognostic biomarker in myocardial infarction.
- Loss of function of NPM1 through antisense oligonucleotide drug or inhibitor NSC348884 might be the potential therapeutic strategy to ameliorate cardiac injury and promote tissue repair after ischemic heart attack.

Nonstandard Abbreviations and Acronyms

AMPK	AMP-activated protein kinase
Arg1	arginase 1
ASO	antisense oligonucleotide
BMDM	bone marrow-derived macrophage
ChIP	chromatin immunoprecipitation
HIF	hypoxia-inducible factor
IL-4	interleukin 4
KDM	histone demethylase
MI	myocardial infarction
mTOR	mechanistic target of rapamycin kinase
NPM1	nucleophosmin 1
OXPHOS	oxidative phosphorylation
PBMC	peripheral blood mononuclear cell
TCA	tricarboxylic acid
TSC1	TSC complex subunit 1
WT	wild type

Myocardial infarction (MI) causes significant cardiomyocyte loss and elicits extensive inflammatory responses. Although these early and appropriate local inflammatory events aid in eliminating cell debris and initiating myocardial repair, the excessive inflammation contributes to the destruction of salvable cardiomyocytes, leading to inefficient wound healing, adverse remodeling, and cardiac dysfunction in patients with MI.[1] Therapeutic interventions that promote infarct healing may suppress the destructive inflammatory process and facilitate a better postinfarct recovery.[2] Macrophages play central roles in both the early inflammatory and subsequent repair phases, which undergo a transition from the proinflammatory phenotype to the reparative one to aid tissue healing during the resolution of acute inflammation.[3] Reparative macrophages, belonging to the M2-like macrophage populations, foster cardiac repair by limiting destructive inflammation, facilitating angiogenesis, and suppressing fibroblast activation and extracellular matrix deposition.[4] Modulating the functional phenotypic transformation of cardiac macrophages may be a promising strategy to protect against adverse cardiac remodeling and heart failure postinfarction. Although some attempts have been made to amplify the reparative macrophage subpopulation in MI, ideal clinical therapeutic effects have not yet been achieved. Thus, it is essential to deeply elucidate the key factor that determines the phenotypic transformation of cardiac macrophages after MI and explore better strategies to enhance their reparative functions.

Macrophages undergo numerous bioenergetic and biosynthetic changes to support their transition to a reparative phenotype. Metabolic adaptation is recognized as a vital characteristic and prerequisite for the transition of macrophage phenotype.[5] Inflammatory macrophages depend on glycolysis for energy production, whereas reparative macrophages use oxidative phosphorylation (OXPHOS) as the primary energy source.[6] Increasing evidence shows that macrophage metabolism can be manipulated to promote tissue repair and combat diseases such as cardiovascular and inflammatory diseases. The shift in metabolic patterns is associated with mitochondrial biogenesis and various signaling pathways, including mTOR (mechanistic targets of rapamycin kinase) and AMPK (AMP-activated protein kinase).[7,8] Activation of the AMPK pathway was found to facilitate macrophage transition toward a reparative phenotype and improve tissue repair through modulating cellular OXPHOS.[7] In contrast, the mTOR signaling is involved in the regulation of glycolysis and protein synthesis, and its activation promotes inflammatory polarization of macrophages.[8] However, the key molecules orchestrating the mTOR pathway and metabolic adaption in cardiac macrophages after MI remain unclear.

Epigenetic programming constitutes a pivotal regulatory mechanism in the modulation of gene expression and cellular behaviors through reversible modifications of genomic DNA and histones. These modifications have the potential to alter the transcriptional output of key metabolic molecules. As a result, epigenetic remodeling leads to cellular metabolism reprogramming.[9] For example, DNA methylation of *FBP1* (fructose-1,6-biphosphatase) promoter was reported to govern the glucose uptake and glycolysis rate of breast cancer cells.[10] The KDMs (histone demethylases), governing gene transcription by removing methyl groups from specific lysine residues on histones, play diverse roles in biological processes, including DNA repair and cell differentiation. Besides, they are critical in modulating cardiac metabolism and diseases. The enzyme JMJD4 (jumonji domain-containing 4) has recently been identified as a contributor to cardiomyocyte metabolic homeostasis. It appears to protect the heart against dilated cardiomyopathy by facilitating degradation of the metabolic enzyme PKM2 (pyruvate kinase M2).[11] Despite these findings, a comprehensive understanding of the underlying epigenetic regulatory networks is still required to develop strategies that manipulate desirable functional phenotype shift of cardiac macrophages. NPM1 (nucleophosmin 1) is a highly conservative protein implicated in a variety of biological processes, including ribosome biogenesis and DNA damage repair.[12] NPM1 is indispensable for embryonic development, and the alteration in its phase behavior may contribute to vascular malformation.[13,14] In addition, it functions as a proto-oncogene or tumor suppressor in multiple types of cancers, including leukemia and breast cancer.[15] As of yet, the role of NPM1 in the epigenetic programming governing metabolic adaption and phenotype transition of cardiac macrophages under the pathological condition of ischemic heart disease remains unclear.

Here, our study discovered that MI-induced upregulation of NPM1 in patients and mice was closely related to adverse cardiac prognostic indicators. Moreover, macrophage-specific deletion of NPM1 (Npm1-cKO) improved cardiac function and tissue repair after MI by polarizing cardiac macrophages toward the reparative phenotype. The oligomeric NPM1 recruited KDM5b to reduce H3K4me3 modification at the promoter of *Tsc1* (*TSC complex subunit 1*) and suppressed its transcription, which, in turn, maintained inflammatory glycolysis and impeded reparative function of cardiac macrophages. The antisense oligonucleotide (ASO) and oligomerization inhibitor targeting NPM1 were validated to be therapeutically effective for MI.

METHODS

Detailed methods are provided in the Supplemental Material. All other data that support the findings of this study are available from the corresponding author on reasonable request.

Human Studies

The peripheral blood mononuclear cell (PBMC) samples were obtained from 58 patients that were clinically diagnosed with acute MI and 7 individuals without any cardiovascular diseases. The diagnosis of acute MI depends on the presence of a rise of cardiac troponin I with at least one value >99th percentile upper reference limit, as well as with one or more of the following markers: ischemia symptoms, new ischemic ECG changes, pathological Q waves in the ECG, evidence of new viable myocardium loss or new abnormal regional wall motion obtained from imaging, or angiography findings of an intracoronary thrombus.[16] The protocol for isolating human PBMCs has been described previously.[17] In brief, human PBMCs were isolated from 5 mL of peripheral venous blood using a Ficoll-Paque solution (Cytiva, Marlborough, MA). All participants gave informed consent. This study was approved by the ethics committee of Renji Hospital, Shanghai Jiao Tong University School of Medicine, and performed according to the criteria set by the Declaration of Helsinki.

Animals

Lyz2-cre mice (B6.129P2-*Lyz2*$^{tm1(cre)Ifo}$/J, Strain No. 004781) were purchased from Jackson Laboratory. The *Npm1*$^{flox/flox}$ mouse was generated by CRISPR-cas9–mediated genome editing. Exons 2 to 6 of the *Npm1* gene (NCBI Reference Sequence NM_008722.3) were selected as the conditional knockout region. The knockout of this region resulted in frameshift of the *Npm1* gene and loss of function of NPM1. *Npm1*$^{flox/flox}$ mice were crossed with *Lyz2-cre* mice to generate *Npm1*$^{flox/flox}$ *Lyz2-cre* mice with NPM1 deletion in macrophages. Wild type (WT) mice (C57BL/6) were purchased from Shanghai Sippr BK Laboratory Animal Company (Shanghai, China). Mice 8 to 12 weeks of age were used for MI surgery. All mice were fed in a homothermic-specific, pathogen-free facility at the Tongji University School of Medicine. Veterinary care and animal experiments were approved by the Animal Care & Use Committee, Tongji University School of Medicine in accordance with the guidelines of the National Health Commission.

Statistical Analysis

Statistical significance was analyzed by GraphPad Prism (version 8) with tests described in the figure legends. The repeat numbers of samples are given in individual figure legends. The results were presented as mean±SD. The representative images were selected on the basis of the mean value after quantitative analysis. Simple linear regression analyses were performed to examine the correlation between *NPM1* expression and other indicators. Pearson correlation analysis was used to calculate the *r* and *P* values of data with normal distribution. Spearman correlation analysis was used to calculate the *r* and *P* values of data distributed abnormally. The unpaired Student *t* test was used for comparison between 2 groups with normally distributed variables. The *P* values of multiple *t* tests or correlation tests were corrected by false discovery rate using the 2-stage step-up method of Benjamini, Krieger, and Yekutieli.[18] The Shapiro-Wilk test was used to ensure that the data were distributed normally, and the Levene test was used to ensure that the variance was equal. The Mann-Whitney test was used to compare 2 groups with variables not normally distributed.

One-way or 2-way ANOVA followed by the Bonferroni post hoc test was used to compare multiple (>2) groups. The comparisons of survival curves were performed using the Log-rank (Mantel-Cox) test. A value of $P<0.05$ was considered statistically significant.

RESULTS

Upregulated NPM1 Correlates With Deteriorated Prognostic Indicators After MI

We first identified 67 differentially expressed transcription factor genes in PBMCs from patients in the acute phase of MI and 1-year after MI through a bioinformatic transcriptome analysis (GSE123342).[19] Among these transcription factors, NPM1 was increased with the highest fold change (Figure 1A). NPM1 was also consistently upregulated in cardiac tissues from patients with ischemic heart diseases (GSE57338) or dilated cardiomyopathy (GSE120895) compared with individuals without heart failure (Figure 1B and 1C).[20,21] Thus, we validated the ischemia-induced upregulation of *NPM1* mRNA (Figure 1D) and protein levels (Figure 1E and 1F) in PBMCs from patients with MI. Besides, the age, sex, and comorbidity between MI and healthy control groups differed insignificantly (Table S1). NPM1 protein was also increased in PBMCs and ischemic cardiac tissues from MI model mice (Figure 1G through 1I). However, NPM1 was barely changed in PBMCs from patients with stressful liver or kidney damage, according to the published RNA sequencing (RNA-seq) data from GEO data set GSE180014 and GSE218048 (Figure S1A and S1B). These results suggest that NPM1 might be specifically involved in the pathological process after the occurrence of MI.

The hypoxia-inducible factor (HIF) family is the central regulator of multiple signaling cascades triggered by MI, including HIF-1α and HIF-2α. Our data revealed a significant positive correlation between *HIF1A* and *NPM1* expression in PBMCs from patients with MI (Figure S1C). In contrast, no significant correlation was observed between *HIF2A* and *NPM1* expression (Figure S1D). To elucidate the mechanisms driving the upregulation of NPM1 expression after MI, we reanalyzed the publicly available chromatin immunoprecipitation sequencing (ChIP-seq) data with a focus on genes targeted by HIF-1α.[22] As expected, HIF-1α bound to the *NPM1* gene promoter proximal to the transcription start site (Figure S1E). However, no binding signal of HIF-2α was observed (Figure S1E). The public ChIP-seq data further revealed the notable binding of JunD and N-MYC at this locus (Figure S1E). Furthermore, the increased mRNA level of *Npm1* in ischemic cardiac tissues of mice with MI was reversed by the administration of HIF-1α–specific inhibitor LW6 (Figure S1F and S1G), indicating that NPM1 could be transcriptionally activated by HIF-1α under infarct conditions.

To further explore the involvement of NPM1 in cardiac recovery, we assessed the relations between *NPM1* expression level in human PBMCs and prognostic indicators of MI, including BNP (natriuretic peptide B), NT-proBNP (N-terminal pro B type natriuretic peptide), cardiac troponin I, CK-MB (creatine kinase M-type), MB (myoglobin), CRP (C-reactive protein), IL-6 (interleukin 6), and IL-1β (interleukin 1β). These molecules have been proven to be strongly associated with the prognosis and severity of MI.[23,24] In patients with MI, *NPM1* mRNA levels exhibited a positive correlation with BNP and NT-proBNP plasma concentrations, both established markers of heart failure severity (Figure 1J and 1K). According to the levels of alanine aminotransaminase 1, aspartate aminotransferase, blood urea nitrogen, and creatinine, there was no hepatic or renal failure in the enrolled patients (Figure S2A). As a result, the potential effects of hepatic and renal diseases on plasma BNP and NT-proBNP could be ruled out. Furthermore, the mRNA levels of *IL6* and *IL1B* in PBMCs positively correlated with the *NPM1* mRNA level (Figure 1L; Figure S2B). However, *ARG1 (Arginase 1)*, a reparative marker of macrophage, was found to be negatively correlated with *NPM1* mRNA expression (Figure S2C). Besides, we also analyzed the expression of several genes mediating cardiac repair after MI, including *GDF15* (growth differentiation factor 15), *MERTK* (myeloid-epithelial-reproductive receptor tyrosine kinase), and *MFGE8* (milk fat globule epidermal growth factor 8),[25,26] and found that these 3 genes were also negatively correlated with *NPM1* mRNA expression (Figure S2D through S2F). Next, we defined patients who had MI with *NPM1* expression levels greater than the median as the group of "$>$Median," and those with *NPM1* levels less than or equal to the median as the group of "$\leq$Median." Although IL-6 and IL-1β levels in plasma differed insignificantly between these 2 groups (Figure S2G), CRP levels in the $>$Median group were significantly higher than those in the $\leq$Median group (Figure 1M). These results suggest that *NPM1* expression in PBMCs is related to excessive inflammatory responses after MI. On the other hand, the plasma levels of cardiac troponin I, CK-MB, and MB in the $>$Median group were also higher than those in the $\leq$Median group (Figure 1N and 1O; Figure S2H). In addition, we reanalyzed the single-cell RNA-seq data (GEO data set GSE145154) from left ventricular tissues in ischemic lesions of patients with MI and nonfailing controls. NPM1 was found to be upregulated in cardiac macrophages of patients with ischemic heart diseases. This upregulation of NPM1 was accompanied by an increase in proinflammatory genes. In contrast, genes indicative of reparative phenotype and function were shown to be decreased (Figure S2I). Immunofluorescence assays provided evidence that NPM1 predominantly localized within the nucleus and exhibited upregulation specifically in cardiac macrophages after MI (Figure 1P and 1Q;

ORIGINAL RESEARCH ARTICLE

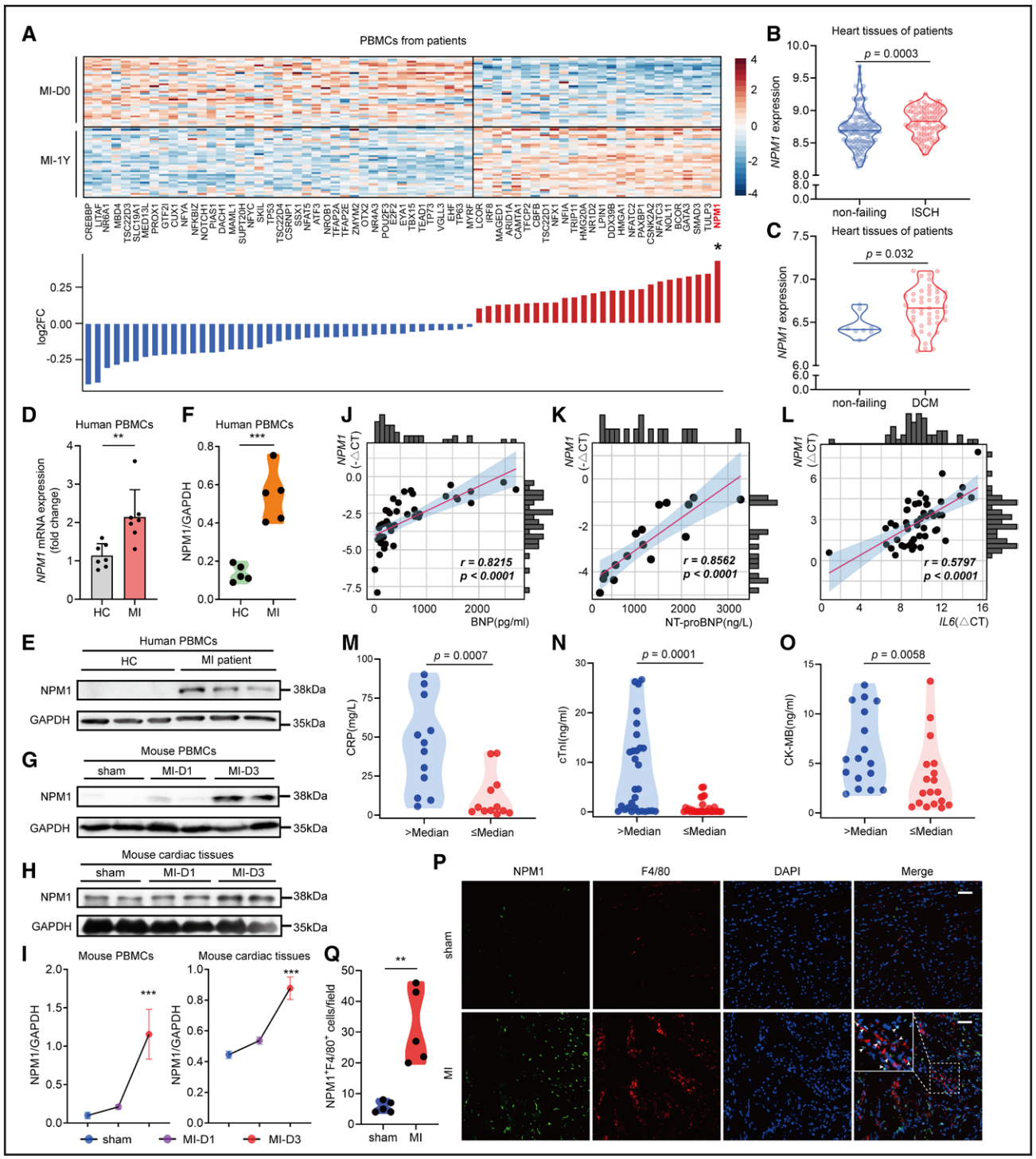

Figure 1. Upregulated NPM1 correlates with adverse prognostic indicators after MI.

A, Reanalysis of transcription factor expression in PBMCs from patients in the acute phase of MI and 1 year after MI (GEO data set GSE123342). *The gene with the highest log_2FC. **B** and **C**, Reanalysis of *NPM1* gene expression in left ventricle tissues from GEO data set GSE57338 (136 nonfailing donors and 95 ischemic heart disease donors; **B**) or in heart tissues from GSE120895 (8 nonfailing donors and 47 dilated cardiomyopathy donors; **C** [Mann-Whitney *U* test]. **D**, Quantitative polymerase chain reaction analysis of *NPM1* mRNA expression in PBMCs of patients with MI or healthy control (HC) individuals (n=7 per group; unpaired Student *t* test). **E** and **F**, Immunoblot analysis (**E**) and quantification (**F**) of NPM1 expression in PBMCs from patients with MI or healthy controls (n=5 per group; unpaired Student *t* test). **G** and **H**, Immunoblot analysis of NPM1 expression in PBMCs (**G**) or ischemic cardiac tissues (**H**) of mice after sham operation or indicated days after MI. **I**, Quantification of immunoblot band intensity in **G** (**left**) and **H** (**right**; n=4 per group; ANOVA followed by Bonferroni test). **J** and **K**, Correlation of *NPM1* mRNA expression in PBMCs with BNP (**J**; n=43) or NT-proBNP (**K**; n=16) levels in plasma of patients with MI. Spearman correlation analysis for **J**, Pearson correlation analysis for **K**. **L**, Correlation between *NPM1* and *IL6* mRNA levels in PBMCs from patients with MI (n=49; Spearman correlation analysis). **M** through **O**, The level of CRP (**M**), cTnI (**N**), or CK-MB (**O**) in plasma of patients who have MI with (*Continued*)

Figure 1 Continued. an *NPM1* level greater than the median compared with patients with an *NPM1* level less than or equal to the median (n=12 per group for **M**; n=29 per group for **N**; n=17 for the >Median group and n=18 for the ≤Median group in **O**; Mann-Whitney *U* test). **P**, Immunofluorescence staining of NPM1 and F4/80 in heart tissues from WT mice after MI or with sham operation (scale bar=50 μm; n=5). **Q**, Quantification of $NPM1^{+}F4/80^{+}$ cells per field of images in **P** (n=5 mice per group; unpaired Student *t* test; $^{**}P<0.01$; $^{***}P<0.001$). BNP indicates natriuretic peptide B; CK-MB, creatine kinase M-type; CRP, C-reactive protein; cTnI, cardiac troponin I; DAPI, 4′,6-diamidino-2-phenylindole; DCM, dilated cardiomyopathy; FC, fold change; ISCH, ischemic heart disease; MB, myoglobin; MI, myocardial infarction; NPM1, nucleophosmin 1; NT-proBNP, N-terminal pro B type natriuretic peptide; and PBMC, peripheral blood mononuclear cell.

Figure S2J). Besides, quantitative assessment of *Npm1* mRNA level in isolated cardiomyocytes, cardiac macrophages, fibroblasts, and endothelial cells from mouse heart tissues validated the findings obtained from immunofluorescence staining (Figure S2K). Taken together, these results demonstrate that the upregulated NPM1 in monocytes/macrophages has a strong correlation with inflammatory responses, cardiac injury, and heart failure after MI stress.

Macrophage-Specific NPM1 Deficiency Alleviates Cardiac Ischemic Injury and Dysfunction

Because NPM1 was predominantly upregulated in cardiac macrophages, macrophage-specific NPM1-deficient mice (*Npm1*$^{flox/flox}$*Lyz2-cre*, termed Npm1-cKO) were generated by crossing *Npm1*$^{flox/flox}$ mice with *Lyz2-cre* mice to investigate the role of NPM1 in cardiac ischemic injury (Figure S3A). The remarkable reduction of NPM1 mRNA and protein expression in Npm1-cKO mice was validated in both cardiac macrophages (Figure S3B and S3C) and bone marrow–derived macrophages (BMDMs) (Figure S3D) compared with *Npm1*$^{flox/flox}$ counterparts (termed WT mice). There was no remarkable difference in the shape and size of the bodies, spleen, thymus, or lymph nodes between WT and Npm1-cKO mice, with comparable body weights (Figure S3E through S3G). NPM1 deficiency had no influence on the development and differentiation of T cells in the thymus, spleen, and lymph nodes (Figure S3H). No difference was observed in the proportions of macrophages and monocytes from bone marrow and spleen between Npm1-cKO mice and WT mice (Figure S3I and S3J). NPM1 deficiency also had no remarkable effect on the in vitro differentiation of BMDMs (Figure S3K). In addition, there was no significant difference in the indicators of cardiac structure and function between Npm1-cKO and WT mice under baseline conditions (Figure S3L and S3M). Finally, Npm1-cKO and WT mice with sham operations did not show any idiopathic myocardial infarction or fibrosis (Figure S3N and S3O).

After MI stress, macrophage-specific Npm1-cKO mice showed a higher survival rate than WT mice at day 48 (Figure S4A). Furthermore, NPM1-deficient mice exhibited enhanced cardiac function, as evidenced by an increased left ventricular ejection fraction (Figure 2A through 2C) and fractional shortening (Figure 2D). The left ventricular volume and left ventricular internal diameter were decreased, whereas the thickness of the interventricular septum was increased in Npm1-cKO mice compared with WT mice post-MI (Figure 2E and 2F; Figure S4B), indicating that NPM1-deficient mice had reduced left ventricular dilatation. Triphenyltetrazolium chloride staining showed a marked reduction of myocardial infarct area in NPM1-deficient mice at day 5 after MI (Figure 2G). Masson trichrome staining revealed that NPM1-deficient mice showed the significantly decreased myocardial scar size, reduced ventricular dilatation, and increased interventricular septum thickness at day 24 after MI (Figure 2H). These data demonstrate that NPM1 deficiency in cardiac macrophages improves cardiac function, ameliorates myocardial ischemic injury, and suppresses myocardial fibrosis, in turn protecting against adverse cardiac remodeling and heart failure after MI.

Macrophage-Specific NPM1 Deficiency Promotes Postinfarction Cardiac Repair

Efficient cardiac repair after heart attack can prevent the progression to heart failure. We next explored the role of NPM1 in ischemic heart repair. As shown in Figure 3A, the amount of α-SMA (α-smooth muscle actin)-positive profibrotic myofibroblasts was substantially reduced, whereas the density of microvessels and capillaries around infarcted lesions was markedly increased in macrophage-specific NPM1-deficient mice (Figure 3A and 3B). Furthermore, the expression levels of profibrotic genes such as *Col1a1* (*Collagen type I alpha 1*) and *Acta2* (*Actin alpha 2 smooth muscle*) were significantly reduced, whereas the mRNA levels of angiogenic molecules such as *Vegfa* (*Vascular endothelial growth factor A*) were notably increased in cardiac tissues of Npm1-cKO mice after MI (Figure 3C). NPM1 deficiency also inhibited the protein expression of Collagen-I, α-SMA, VEGFR2, and MFGE8 in ischemic heart tissues after MI (Figure 3D and Figure S5A). In addition, the apoptosis of cardiomyocytes around the ischemic lesions at day 3 after MI was alleviated by NPM1 deletion in macrophages (Figure S5B and S5C). These data indicate that NPM1 deficiency enhanced angiogenesis and inhibited cardiomyocyte apoptosis and excessive cardiac fibrosis.

We further observed the effect of NPM1 deficiency on inflammation resolution in cardiac tissue after MI. Immunofluorescence staining did not show the difference

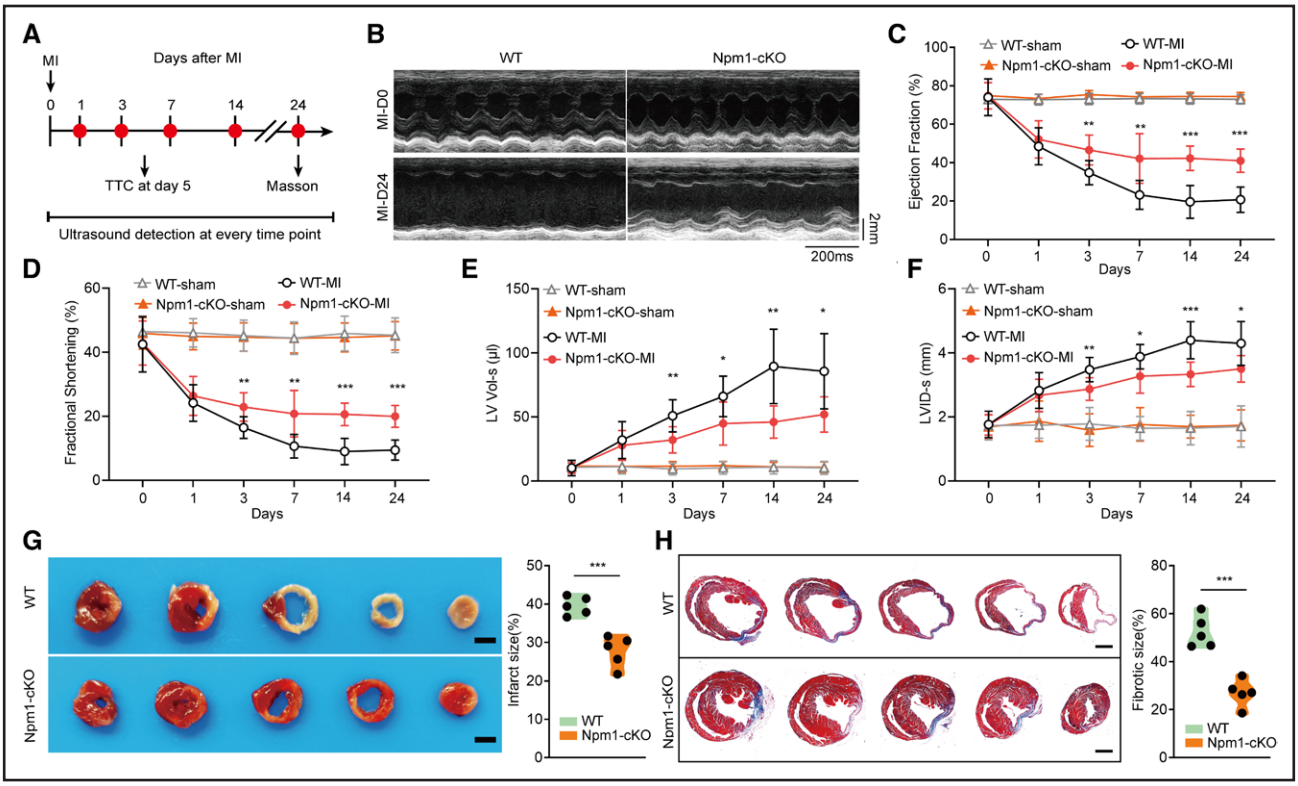

Figure 2. Macrophage-specific NPM1 deficiency ameliorates cardiac dysfunction and adverse remodeling.
A, Experimental design depicting analysis of TTC, Masson trichrome staining, and ultrasound at the indicated days in Npm1-cKO and WT control mice subjected to MI. **B**, Representative M-mode echocardiograms obtained from WT and Npm1-cKO mice at day 0 and day 24 after MI. **C** through **F**, Echocardiographic measurements of left ventricular ejection fraction (**C**), fractional shortening (**D**), systolic left ventricular volume (LV Vol-s; **E**), and systolic LV internal diameter (LVID-s; **F**) in WT and Npm1-cKO mice at the indicated days after MI or sham operation (n=11 per group; 2-way ANOVA followed by Bonferroni test). **G**, TTC staining of sequential cardiac sections from WT and Npm1-cKO mice at day 5 after MI and the quantified size of infarct area (n=5 per group; unpaired Student *t* test). Scale bar=2 mm. **H**, Masson trichrome staining of sequential heart sections from WT and Npm1-cKO mice at day 24 after MI, and the quantified size of fibrotic areas (n=5 per group; unpaired Student *t* test. Scale bar=1 mm. **P*<0.05; ***P*<0.01; ****P*<0.001. MI indicates myocardial infarction; NPM1, nucleophosmin 1; TTC, triphenyltetrazolium chloride; and WT, wild type.

of macrophage infiltration in heart tissues around the infarct lesions between WT and Npm1-cKO mice after MI (Figure S5D and S5E). Furthermore, the populations of infiltrated macrophages, neutrophils, and T cells in ischemic heart tissues of Npm1-cKO and WT mice at day 1 (Figure S5F) and day 3 (Figure S5G) after MI were comparable (Figure S5H), suggesting that NPM1 deficiency did not affect the infiltration of immune cells. Nevertheless, the expression levels of proinflammatory genes (eg, *Tnf*, *Il6*, and *Il1b*) and characteristic genes of M1 macrophages (eg, *Nos2* and *Cd86*) were significantly decreased in cardiac tissues of Npm1-cKO mice at day 3 and day 5 after MI (Figure 3E; Figure S5I). In addition, NPM1 deficiency markedly upregulated the expression of characteristic genes of reparative macrophages including *Arg1*, *Chil3* (chitinase-like 3), *Mrc1* (mannose receptor C-type 1), *Retnla* (resistin-like alpha), and *Il10* in cardiac tissues at day 3 and day 5 after MI (Figure 3F; Figure S5J). Of note, some functional molecules that contributed to cardiac repair were markedly elevated in cardiac tissues of Npm1-cKO mice after MI, including *Mertk*, *Mfge8*, *Gdf15*, *Cnpy2* (Canopy FGF signaling regulator 2), and *Tmsb4x* (Thymosin beta 4 X-linked; Figure 3G).[27,28] In contrast, NPM1 deficiency reduced the expression of genes such as *Hpgd* (hydroxyprostaglandin dehydrogenase 15) in cardiac tissues after infarction, which are detrimental to the repair of damaged tissues (Figure 3H).[29] Consistent with the mRNA level, the plasma GDF15 level was also increased by NPM1 deficiency (Figure 3I). NPM1 knockout increased the population of MFGE8-positive reparative macrophages in the ischemic cardiac tissues (Figure 3J). These results indicate that NPM1 deficiency facilitates inflammation resolution, enhances angiogenesis, and promotes tissue repair after heart attack by boosting the expression and secretion of reparative molecules.

NPM1 Deficiency Enhances Reparative Phenotype of Cardiac Macrophages

Reparative macrophages have been reported to protect hearts against ischemic injury and pathological fibrosis through producing various cardioprotective functional factors and promoting angiogenesis.[26] We next investigated

 Circulation. 2024;149:1982–2001. DOI: 10.1161/CIRCULATIONAHA.123.065506

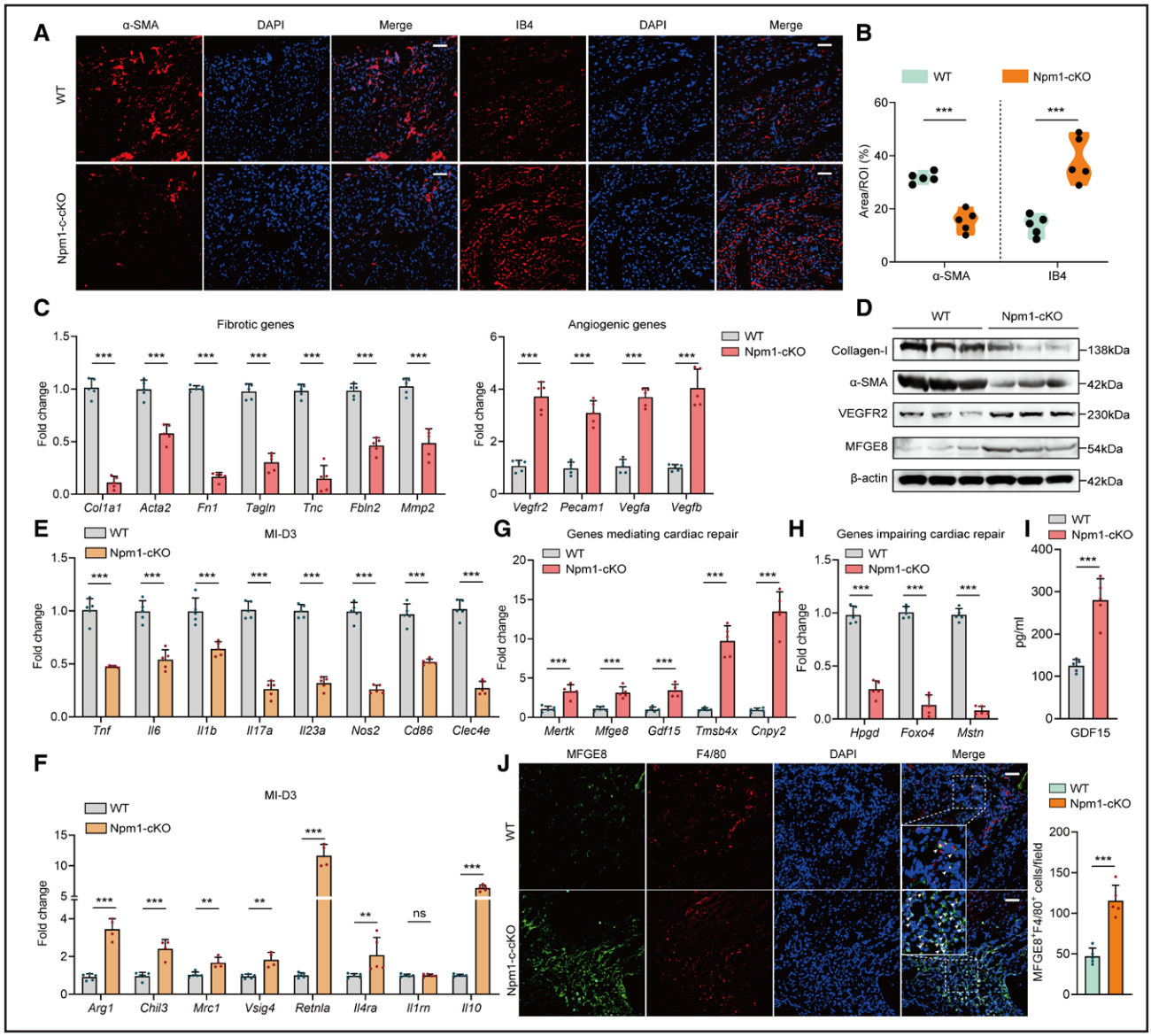

Figure 3. NPM1 deficiency in cardiac macrophages suppresses fibrotic reaction and facilitates angiogenesis and cardiac repair after MI.

A, Immunofluorescence staining of α-SMA and isolectin-B4 (IB4) in ischemic heart tissues of mice at day 24 after MI. Scale bar=50 μm. **B**, Quantitative data for the area/ROI of images in **A** (n=5 per group). **C**, The mRNA expression levels of genes associated with cardiac fibrosis and angiogenesis in ischemic heart tissues of WT and Npm1-cKO mice at day 14 after MI (n=5 per group). **D**, Immunoblot analysis of Collagen-I, α-SMA, VEGFR2, and MFGE8 protein levels in ischemic heart tissues of WT and Npm1-cKO mice at day 14 after MI (n=3 per group). **E** and **F**, The mRNA expression levels of genes indicative of proinflammatory (**E**) and reparative (**F**) phenotypes in ischemic heart tissues of WT and Npm1-cKO mice at day 3 after MI (n=5 per group). **G** and **H**, The mRNA expression levels of genes mediating (**G**) or impairing (**H**) myocardial repair in ischemic heart tissue of WT and Npm1-cKO mice at day 5 after MI (n=5/group). **I**, ELISA measurement of the plasma GDF-15 levels of WT and Npm1-cKO mice at day 5 post-MI (n=5/group). **J**, Immunofluorescence staining and quantification of the amounts of MFGE8$^+$ macrophages in the cardiac tissues of WT and Npm1-cKO mice at day 5 after MI. Scale bar=50 μm. Unpaired Student *t* test for **C** through **J**. $^{**}P<0.01$; $^{***}P<0.001$. ns indicates not significant. DAPI indicates 4′,6-diamidino-2-phenylindole; GDF-15, growth differentiation factor 15; MFGE8, milk fat globule epidermal growth factor 8; NPM1, nucleophosmin 1; ROI, region of interest; α-SMA, α-smooth muscle actin; VEGFR2, vascular endothelial growth factor 2; and WT, wild type.

the effect of NPM1 on the phenotype and function of cardiac macrophages. F4/80$^+$Ly6C^{low} macrophages with Arg1-positive expression were defined as reparative macrophages. Immunofluorescence staining showed the markedly upregulated Arg1 expression in F4/80$^+$ macrophages of ischemic cardiac tissue (Figure 4A and 4B), and flow cytometry analysis showed the obviously increased proportion of F4/80$^+$Ly6C^{low} reparative macrophages and the decreased proportion of F4/80$^+$Ly6C^{high} inflammatory macrophages in cardiac tissue from NPM1-deficient mice at day 5 after MI (Figure 4C and 4D). Consistent with the expanded cell population of cardiac

ORIGINAL RESEARCH ARTICLE

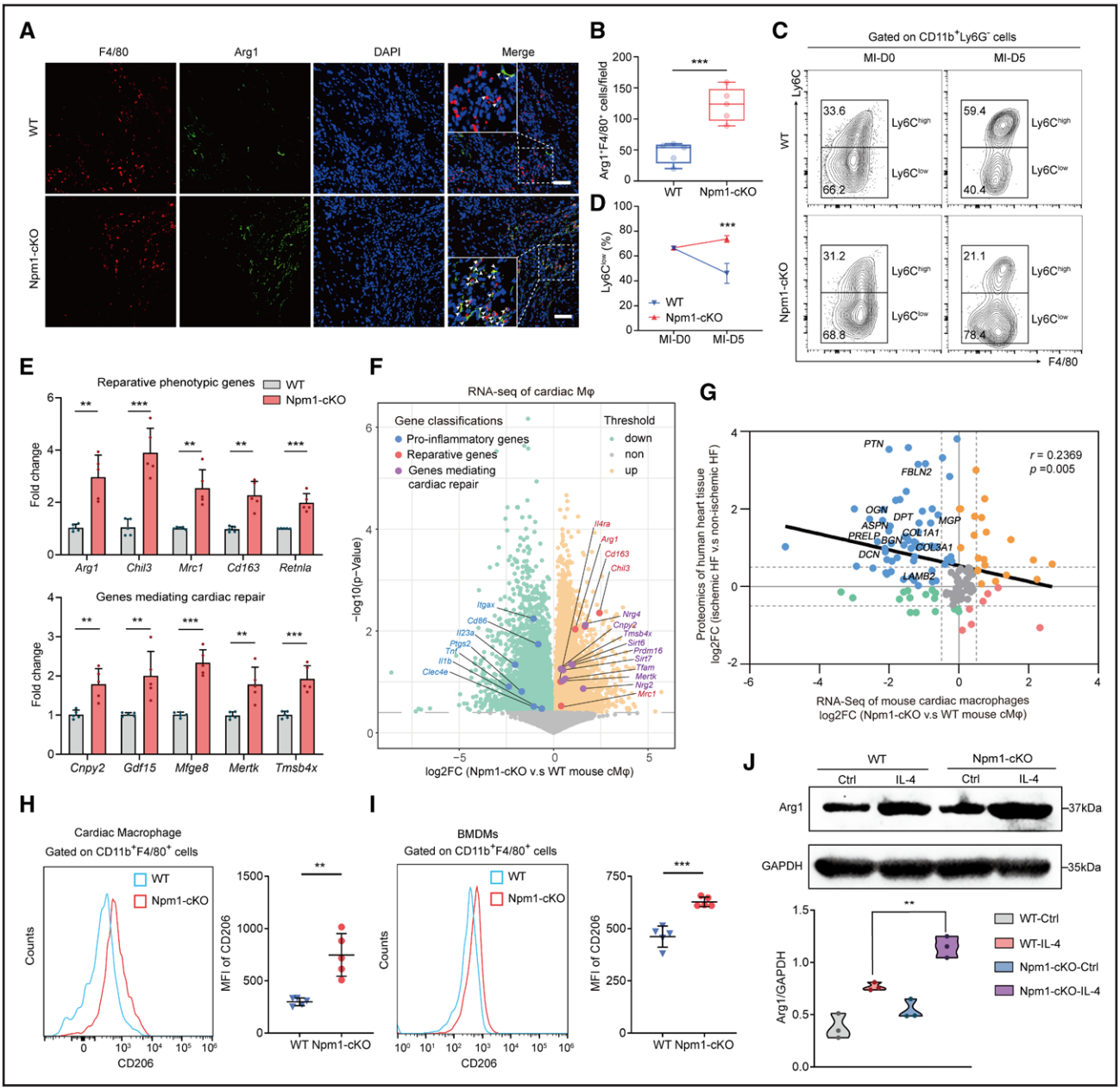

Figure 4. NPM1 deficiency enhances reparative phenotype of cardiac macrophages.

A and **B**, Immunofluorescence staining (**A**) and quantification (**B**) for analyzing the amounts of reparative macrophages ($F4/80^+Arg1^+$) in the border zone of heart tissues from WT and Npm1-cKO mice at day 5 after MI. Scale bar=50 μm (n=5 per group; unpaired Student *t* test. **C** and **D**, Flow cytometry analyses (**C**) and quantification (**D**) of reparative macrophages ($F4/80^+Ly6C^{low}$) in heart tissues from WT and Npm1-cKO mice at day 0 and day 5 after MI (n=5 per group; ANOVA followed by Bonferroni post hoc test). **E**, The mRNA expression levels of reparative phenotypic markers (**top**) and genes mediating cardiac repair (**bottom**) in cardiac macrophages isolated from heart tissues of WT and Npm1-cKO mice at day 5 after MI (n=5 per group; unpaired Student *t* test). **F**, Volcano plot from RNA-seq data of the expression of genes indicative of macrophage phenotypes and reparative function in cardiac macrophages isolated from WT and Npm1-cKO mice at day 5 after MI (n=4 per group). **G**, Simple linear regression analysis of the fibrotic proteins changed in cardiac tissues of patients with ischemic heart failure (data obtained from Barallobre-Barreiro et al[30]) and the differentially expressed genes in cardiac macrophages from Npm1-cKO MI mice compared with WT MI mice. **H**, Flow cytometry analysis and quantification of CD206 expression in cardiac macrophages from WT and Npm1-cKO mice at day 5 after MI (n=5 per group; unpaired Student *t* test). **I**, Flow cytometry analysis and quantification of CD206 expression in BMDMs isolated from WT and Npm1-cKO mice followed by IL-4 stimulation for 24 hours (n=5 per group; unpaired Student *t* test). **J**, Immunoblot analysis and quantification of Arg1 protein level in WT and Npm1-cKO BMDMs stimulated with IL-4 for 24 hours (n=3 per group; ANOVA followed by Bonferroni test). Box-and-whisker plots: the box extends from the 25th to 75th percentiles; whiskers depict minimal to maximal values. $^{**}P<0.01$; $^{***}P<0.001$. Arg1 indicates Arginase 1; BMDM, bone marrow–derived macrophage; Ctrl, control; DAPI, 4′,6-diamidino-2-phenylindole; FC, fold change; HF, heart failure; IL-4, interleukin 4; MFI, mean fluorescence intensity; MI, myocardial infarction; NPM1, nucleophosmin 1; RNA-seq, RNA sequencing; and WT, wild type.

reparative macrophages, the expression levels of multiple reparative and cardioprotective genes, including *Arg1*, *Chil3*, *Gdf15*, and *Mertk*, were significantly upregulated, whereas the expression levels of inflammation-related genes such as *Nos2* and *Il6* were downregulated in cardiac macrophages isolated from Npm1-cKO mice after MI (Figure 4E; Figure S6A). RNA-seq analysis further consistently certified that a broad range of genes indicative of reparative phenotype and function were markedly upregulated in cardiac macrophages isolated from heart tissues of Npm1-cKO mice compared with those from WT mice after MI, whereas the expression levels of multiple inflammatory genes were inhibited in Npm1-cKO cardiac macrophages (Figure 4F). Of note, the upregulated functional genes, such as *Mertk*, *Cnpy2*, *Tmsb4x*, *Tfam* (Transcription factor A mitochondrial), Neuregulin (*Nrg*), and Sirtuin (*Sirt*), have been reported to support the clearance of damaged cells, reduce excessive inflammation and fibrosis, enhance neovascularization, improve mitochondrial function, and promote cardiomyocyte survival, ultimately facilitating the reparative process after MI.[31–33] These results indicate that NPM1-deficient cardiac macrophages display the enhanced reparative phenotype and function without proinflammatory characteristics. Furthermore, a substantial decrease in the enrichment of gene sets associated with TGF-β (transforming growth factor β) signaling and extracellular matrix receptor interaction pathway was observed in Npm1-cKO cardiac macrophages (Figure S6B). The analysis of proteomic data from heart tissues of patients with ischemic or nonischemic heart failure showed that a series of upregulated proteins in patients with ischemic heart failure emerged to be responsible for ischemia-induced extracellular matrix generation and formation (Figure 4G).[30] However, the upregulation of these extracellular matrix–related molecules in patients with ischemic heart failure was almost all reversed in Npm1-cKO cardiac macrophages (Figure 4G; Figure S6C). The changes of these molecules in these human proteomic data and our RNA-seq data of mouse cardiac macrophages were significantly negatively correlated in the combined analysis, suggesting that NPM1-deficient cardiac macrophage–mediated tissue repair prevents pathological myocardial fibrosis. Furthermore, an apparent expansion of the regulatory T-cell population was observed in Npm1-cKO heart tissue at day 5 after MI, suggesting that another protective function exists in NPM1-deficient reparative macrophages (Figure S6D). The representative phenotype markers of reparative macrophages, CD206 and Arg1, were not only upregulated in cardiac macrophages isolated from Npm1-cKO mice after MI (Figure 4H), but also increased in NPM1-deficient BMDMs treated with IL-4 (interleukin 4; Figure 4I and 4J). Taken together, these data indicate that NPM1 deficiency polarizes cardiac macrophages to the reparative phenotype and strengthens their tissue repair capabilities.

NPM1 Deficiency Facilitates OXPHOS Remodeling of Reparative Macrophages Through the mTOR Pathway

A recent study found that NPM1 could regulate the effector capacity of macrophages through mediating ribosome dysregulation.[34] Therefore, we silenced the NPM1-interacting rRNA 2′-*O*-methyltransferase FBL (fibrillarin) to investigate whether NPM1 regulated reparative cardiac macrophage function through 2′-*O*-methylation. However, FBL silencing had no effect on NPM1 deficiency–induced upregulation of reparative phenotypic markers in macrophages, including *Arg1* and *Mrc1* (Figure S7A), excluding the possibility that FBL-mediated 2′-*O*-methylation and ribosome dysfunction are involved in NPM1-mediated function regulation of reparative cardiac macrophages. Cellular metabolism, especially OXPHOS, has been reported to support the reparative function of macrophages in various ischemic and tissue injury diseases. Next, we investigated whether metabolism reprogramming was involved in the phenotypic transition of cardiac macrophages mediated by NPM1 deficiency. Metabolic flux assay exhibited the boosted basal oxygen consumption rate and maximum respiratory capacity in both resting and IL-4–activated NPM1-deficient macrophages (Figure 5A). Nevertheless, the significantly reduced basal extracellular acidification rate and maximal glycolysis capacity were found in NPM1-deficient macrophages compared with WT cells (Figure 5B). As identified by targeted central carbon metabolomic profiling, several metabolites of the top 20 differentially expressed metabolites were involved in the tricarboxylic acid (TCA) cycle (Figure 5C). The TCA cycle also enriched the most abundant differential metabolites (Figure 5D). Besides, most of the metabolites involved in the TCA cycle were upregulated, whereas succinic acid, a metabolite that promotes inflammation, was decreased in NPM1-deficient macrophages (Figure 5E). The data from α-ketoglutaric acid, succinic acid, and citric acid assays were consistent with the metabolomic profiling and showed that the α-ketoglutaric acid/succinic acid ratio was increased in Npm1-cKO macrophages, which was previously proved to be a characteristic of reparative phenotypic transition (Figure S7B). In addition, the expression levels of enzymes, including *Pdha1* (pyruvate dehydrogenase E1 alpha 1), *Idh1* (isocitrate dehydrogenase 1), and *Sdhd* (succinate dehydrogenase complex subunit D), which participate in regulating the TCA cycle, were increased in IL-4–treated Npm1-cKO macrophages, compared with the WT group (Figure S7C). Consistent with the strengthened TCA cycle, the genes involved in the electron transport chain complex I to V were upregulated in NPM1-deficient cardiac macrophages isolated from the mouse heart at day 5 after MI (Figure 5F; Figure S7D). These results demonstrate that mitochondrial OXPHOS is enhanced, whereas aerobic glycolysis is inhibited in NPM1-deficient macrophages.

ORIGINAL RESEARCH ARTICLE

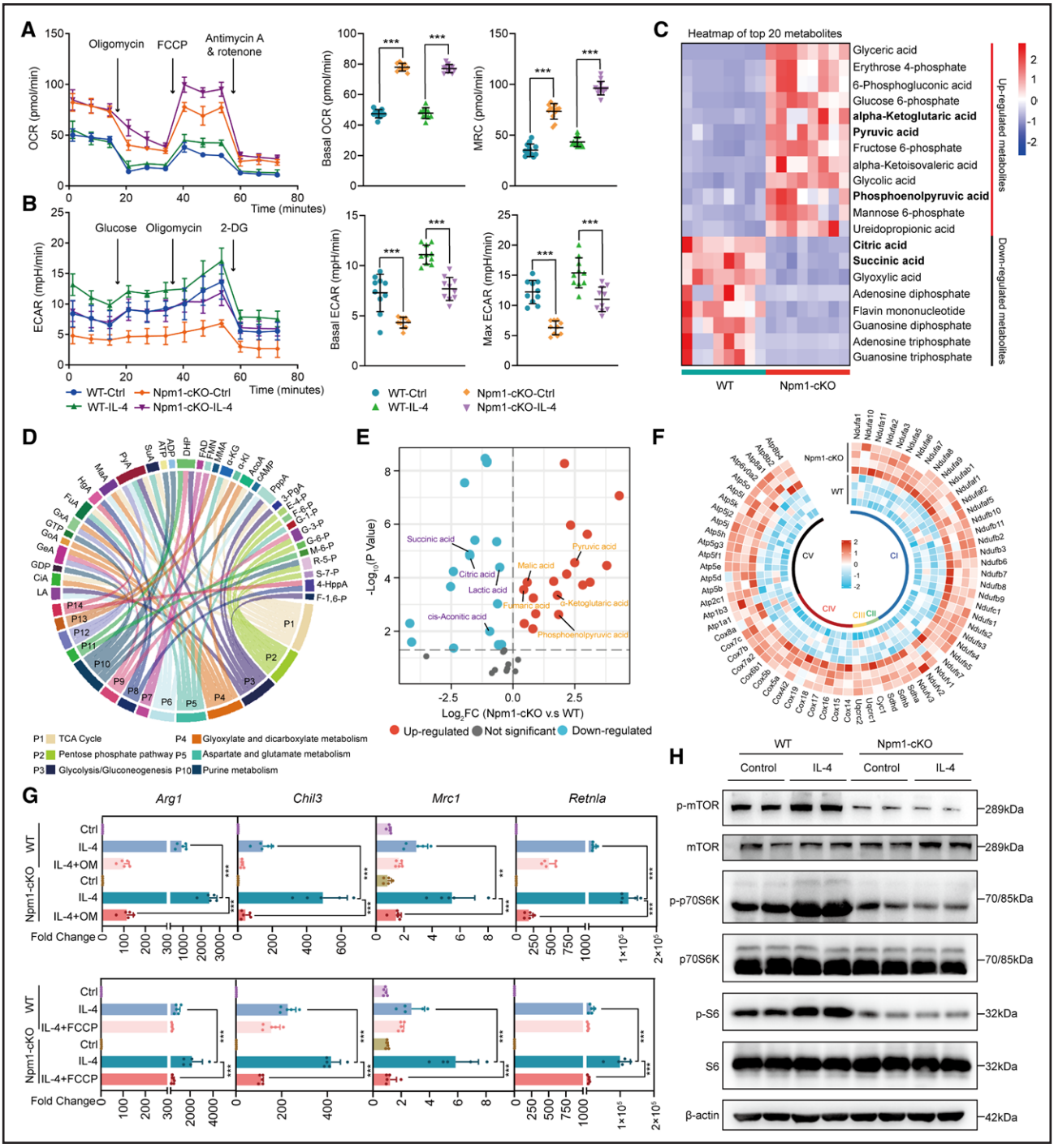

Figure 5. NPM1 deficiency promotes oxidative phosphorylation reprogramming of reparative macrophages through the mTOR pathway.

A, Summarized OCR tracing, basal OCR, and maximal respiratory capacity in Npm1-cKO and WT BMDMs stimulated with IL-4 for 24 hours or left untreated. **B**, Summarized ECAR tracing, basal ECAR, and maximal ECAR in Npm1-cKO and WT BMDMs stimulated with IL-4 for 24 hours or left untreated (n=10 per group; 2-way ANOVA followed by Bonferroni test). **C**, Heatmap depicted the top 20 differential metabolites in IL-4–stimulated Npm1-cKO BMDMs compared with WT BMDMs (n=8 per group). **D**, Chordal graph revealed the pathway enrichment of differential metabolites, as identified by metabolome profiling, in IL-4–stimulated Npm1-cKO BMDMs compared with WT BMDMs. AcoA indicates *cis*-aconitic acid; ADP, adenosine 5′-diphosphate; ATP, adenosine 5′-triphosphate; c-AMP, cyclic adenosine monophosphate; CiA, citric acid; DHP, dihydroxyacetone phosphate; E-4-P, erythrose 4-phosphate; F-6-P, fructose 6-phosphate; F-1,6-P, fructose 1,6-bisphosphate. FAD, flavin adenine dinucleotide; FMN, flavin mononucleotide; FuA, fumaric acid; G-1-P, glucose 1-phosphate; G-3-P, glycerol 3-phosphate; G-6-P, glucose 6-phosphate; GDP, guanosine 5′-diphosphate; GeA, glyceric acid; GoA, glyoxylic acid; GTP, guanosine 5′-triphosphate; GxA, glyoxylic acid; HgA, homogentisic acid; 4-HppA, 4-hydroxyphenylpyruvic acid; α-KG, α-ketoglutaric acid; α-KI, α-ketoisovaleric acid; LA, lactic acid; M-6-P, mannose 6-phosphate; MaA, malic acid; MMA, methylmalonic acid; 3-PgA, 3-phosphoglyceric acid; PppA, phosphoenolpyruvic acid; PyA, pyruvic acid; R-5-P, ribose 5-phosphate; S-7-P, sedoheptulose 7-phosphate; and SuA, succinic acid. **E**, The volcano plot displayed the (*Continued*)

Figure 5 Continued. magnitude and significance of altered metabolites associated with TCA cycle in IL-4–treated Npm1-cKO BMDMs compared with WT BMDMs. **F**, Heatmap from RNA-seq data of genes related to mitochondrial electron transfer chain complexes in cardiac macrophages isolated from WT and Npm1-cKO mice at day 5 post-MI (n=4 per group). **G**, The mRNA expression levels of genes indicative of reparative phenotype in Npm1-cKO and WT BMDMs left untreated or treated with IL-4 alone, the combination of IL-4 and OM, or the combination of IL-4 and FCCP (n=5 per group; 2-way ANOVA followed by Bonferroni test). **H**, Immunoblot analysis of phosphorylated (p)-mTOR, total-mTOR, p-P70S6K, total-P70S6K, p-S6 protein, and total-S6 protein levels in Npm1-cKO and WT BMDMs with or without IL-4 stimulation. $^{**}P<0.01$; $^{***}P<0.001$. BMDM indicates bone marrow–derived macrophage; Ctrl, control; 2-DG, 2-deoxy-D-glucose; ECAR, extracellular acidification rate; FC, fold change; FCCP, carbonyl cyanide 4-(trifluoromethoxy) phenylhydrazone; IL-4, interleukin 4; mTOR, mechanistic target of rapamycin kinase; NPM1, nucleophosmin 1; OCR, oxygen consumption rate; OM, oligomycin; TCA, tricarboxlic acid; and WT, wild type.

We further treated BMDMs with OXPHOS inhibitors, oligomycin and carbonyl cyanide 4-(trifluoromethoxy) phenylhydrazone to observe the expression change of characteristic genes in IL-4–treated reparative macrophages. The reversion of increased reparative gene expression mediated by oligomycin and carbonyl cyanide 4-(trifluoromethoxy) phenylhydrazone validated the necessity of the boosted OXPHOS metabolism reprogramming for NPM1 deficiency–mediated transition toward reparative phenotype in macrophages (Figure 5G). The mTOR pathway is one of key signaling pathways influencing energy metabolism.[35,36] Immunoblot assay showed that the phosphorylation levels of mTOR, p70S6K, and S6 proteins were suppressed in Npm1-cKO BMDMs (Figure 5H). Overall, these findings indicate that NPM1 deficiency shifts metabolic status from glycolysis to OXPHOS by inhibiting mTOR signaling, which is required for the polarization of macrophages toward a reparative phenotype.

NPM1 Targets TSC1 to Polarize the Phenotype of Cardiac Macrophages

We then sought to identify the direct target gene by which NPM1 modulated the activation of mTOR pathway. As indicated by RNA-seq and quantitative polymerase chain reaction analysis data of cardiac macrophages isolated from Npm1-cKO mice and WT mice at day 3 after MI, *TSC1*, a crucial suppressor of mTOR pathway, was the most upregulated gene among all the genes involved in the mTOR pathway (Figure 6A and 6B). The protein and mRNA levels of TSC1 were also raised in Npm1-cKO BMDMs, compared with WT BMDMs, after IL-4 treatment (Figure 6C and 6D). Furthermore, TSC1 silencing could reverse the upregulated expression of reparative markers, including *Arg1*, *Mrc1*, *Chil3*, and *Retnla*, induced by IL-4 in Npm1-cKO BMDMs (Figure 6E and 6F), indicating that TSC1 was essential for NPM1-mediated phenotypic transition of macrophages.

Considering the established role of NPM1 as a transcription regulator, we proposed that NPM1 may bind to *Tsc1* promoter for transcription regulation. We validated the homology of the *TSC1* promoter among *Homo sapiens*, *Mus musculus*, and other mammalian animals. The similarity between *H sapiens* and *M musculus* was mostly >70% (Figure S8A). The published assay for transposase-accessible chromatin using sequencing data (GSM2867759) was used to identify the open chromatin regions of *Tsc1* promoter in BMDMs (Figure 6G).[37] Cut&Tag analysis in primary cardiac macrophages found that the binding site of NPM1 was located between −260 bp and +220 bp in the accessible region of *Tsc1* promoter, and the enrichment of NPM1 to *Tsc1* promoter was significantly increased in cardiac macrophages from infarcted hearts (Figure 6G). The analysis results of the published ChIP-seq data about histone methylation or acetylation in BMDMs showed that only the specific peak of H3K4me3 but not H3K27me3 existed at the binding site of NPM1 in *Tsc1* promoter, which was compatible with the open chromatin region of *Tsc1* promoter displayed in the assay for transposase-accessible chromatin using sequencing results (Figure 6G).[38–40] The enhanced specific binding of NPM1 to *Tsc1* promoter induced by IL-4 in BMDMs was indicated by Cut&Tag analysis (Figure 6G). In addition, the data from ChIP-quantitative polymerase chain reaction using the fragments of *Tsc1* promoter confirmed that the NPM1 binding site on *Tsc1* promoter was situated between −260 bp and +220 bp (Figure 6H). In addition, NPM1 did not bind the promoters of other potential target genes, including *Tsc2*, *Arg1*, and *Mrc1* (Figure S8B). All together, these data indicate that NPM1 can specifically bind to *Tsc1* promoter and suppress *Tsc1* expression, thereby enhancing mTOR pathway activation in macrophages.

Oligomeric NPM1 Recruits KDM5b to Restrain the H3K4me3 Modification and Transcription of TSC1

Next, we investigated whether NPM1 regulated histone modifications to control *Tsc1* transcription. Cut&Tag assay found that histone H3K4me3 level was markedly increased by NPM1 deficiency in post-MI cardiac macrophages and in IL-4–activated BMDMs (Figure 7A), which was verified in Npm1-cKO BMDMs treated with IL-4 through ChIP-quantitative polymerase chain reaction (Figure 7B). However, NPM1 did not affect histone H3K9me3 or H3K27me3 methylation modification at the *Tsc1* promoter (Figure S9A). Because NPM1 had no histone demethylation activity, we proposed that it might recruit a histone demethylase. The KDM5 family members and KDM2b have been demonstrated to regulate

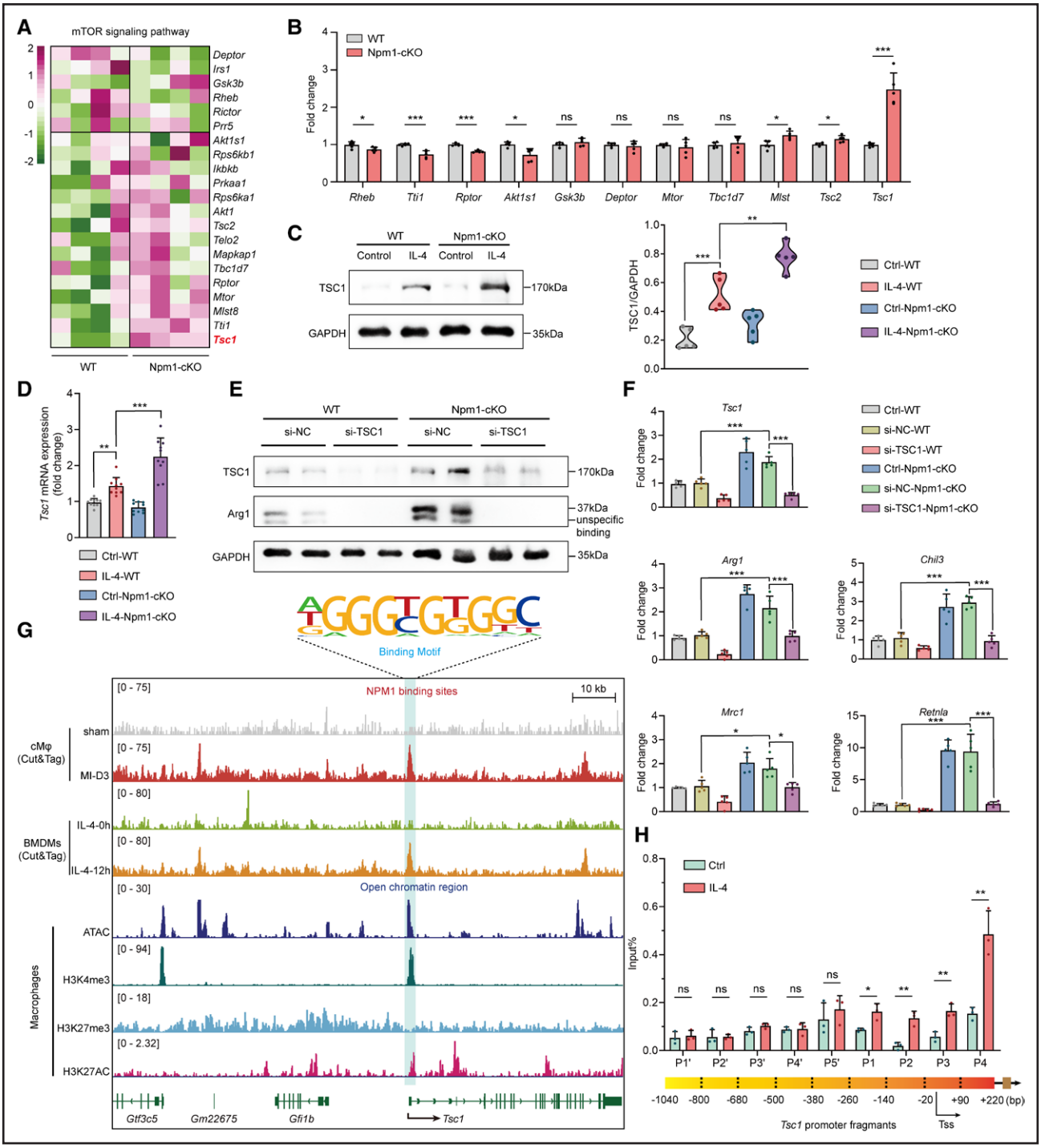

Figure 6. NPM1 targets TSC1 to mediate phenotypic transition of cardiac macrophages.

A, Heatmap of differentially expressed genes in the mTOR signaling pathway, identified by RNA sequencing of cardiac macrophages isolated from Npm1-cKO and WT mice at day 3 after MI (n=4 per group). **B**, The mRNA expression levels of genes in the mTOR signaling pathway detected by quantitative polymerase chain reaction in cardiac macrophages isolated from Npm1-cKO and WT mice at day 3 after MI (n=5 per group; unpaired Student *t* test). **C** and **D**, Immunoblot analysis of TSC1 protein level (n=3 per group) or quantitative polymerase chain reaction analysis of *Tsc1* mRNA level (n=10 per group) in Npm1-cKO and WT BMDMs treated with IL-4 for 24 hours or left untreated (ANOVA followed by Bonferroni test). **E**, Immunoblot analysis of TSC1 and Arg1 protein levels in Npm1-cKO and WT BMDMs transfected with siRNA targeting *Tsc1* (si-TSC1) or negative control siRNA (si-NC) followed by IL-4 treatment for 24 hours. **F**, Quantitative polymerase chain reaction analysis of mRNA levels of *Tsc1* and other genes indicative of reparative phenotype in Npm1-cKO and WT BMDMs transfected as in **E** followed by IL-4 treatment for 24 hours (n=5 per group; ANOVA followed by Bonferroni test). **G**, Integrative Genomics Viewer analysis of NPM1 binding signal in the gene locus of *Tsc1*. Cut&Tag assays for NPM1 binding were performed in cardiac macrophages from mice with sham operation or at day 3 after MI and in WT mouse BMDMs with IL-4 treatment for 0 or 12 hours. Integrative Genomics Viewer analysis of assay for transposase-accessible chromatin using sequencing (GSM2867759), H3K4me3 (GSM1692805), H3K27me3 (GSM1692804), and H3K27AC (*Continued*)

 Circulation. 2024;149:1982–2001. DOI: 10.1161/CIRCULATIONAHA.123.065506

Figure 6 Continued. signal (GSM2060963) in WT mouse BMDMs in the gene locus of *Tsc1*. **H**, Chromatin immunoprecipitation followed by quantitative polymerase chain reaction analysis of NPM1 enrichment at the promoter of *Tsc1* in WT BMDMs treated with IL-4 for 24 hours or left untreated (n=3 per group; Student *t* test). **P*<0.05; ***P*<0.01; ****P*<0.001. Arg1 indicates Arginase 1; ATAC, transposase-accessible chromatin using sequencing; BMDM, bone marrow–derived macrophage; Ctrl, control; IL-4, interleukin 4; MI, myocardial infarction; mTOR, mechanistic targets of rapamycin kinase; NPM1, nucleophosmin 1; ns, not significant; si-, small interfering; TSC1, TSC complex subunit 1; Tss, transcription start site; and WT, wild type.

the H3K4me3 modification.[41] The published single-cell sequencing dataset (GSE247139) of cardiac tissues from mice subjected to sham operation and MI revealed significant changes in the expression levels of KDM5 family and KDM2b in CD68$^+$ cardiac macrophages after ischemic injury (Figure S9B). Besides, the immunoprecipitation assay indicated that KDM5b but not KDM5a, KDM5c, KDM5d, or KDM2b could interact with NPM1 in both HEK293T cells and macrophages, and this binding was considerably enhanced after IL-4 treatment (Figure 7C; Figure S9C and S9D). The recruitment of KDM5b to *Tsc1* promoter was severely impaired in Npm1-cKO BMDMs (Figure 7D). Furthermore, NPM1 deficiency did not markedly affect the genome-wide chromatin binding of KDM5b (Figure S9E). This infers that NPM1 can interact with KDM5b in a gene-specific manner. In addition, the Re-ChIP assay showed that NPM1 and KDM5b formed a protein complex to bind *Tsc1* promoter in IL-4–activated BMDMs (Figure 7E). Although earlier studies have shown that KDM5b, a H3K4me3 demethylase, can influence transcriptional initiation, elongation, and RNA splicing,[42] our data did not show any significant alteration in a variety of alternative splicing events, implying that NPM1 did not affect global alternative splicing (Figure S9F). In addition, NPM1 did not influence the alternative splicing of *Tsc1* before mRNA (Table S2). Corroborating with the previous study, we observed the elevated enrichments of both total RNA polymerase II and serine 2 phosphorylated RNA polymerase II near the transcription start site of *Tsc1* in Npm1-cKO macrophages compared with WT macrophages, which indicated a significant enhancement of transcriptional elongation (Figure S9G).[42] To elucidate the functional domain that mediated the interaction of NPM1 with KDM5b, different mutants with functional domain deletions were generated to perform co-immunoprecipitation assays (Figure 7F). NPM1 contains the oligomerization domain, acid domain, and RNA binding domain. The interaction between NPM1 and KDM5b was blocked by deletion of the oligomerization domain of NPM1 or by deletion of the JmjC demethylase activity domain of KDM5b (Figure 7G). IL-4 treatment did not change NPM1 expression or influence its nuclear location (Figure S9H). Oligomer formation was demonstrated to increase the biological activity of NPM1.[43] IL-4 was able to induce NPM1 oligomerization in macrophages, which was disrupted by treatment with NSC348884, the inhibitor of NPM1 oligomerization (Figure 7H). Furthermore, the NPM1-mediated KDM5b recruitment to *Tsc1* promoter was impaired and the H3K4me3 level at *Tsc1* promoter was elevated in IL-4–activated macrophages treated with NSC348884 (Figure 7I and 7J). In addition, NPM1 deletion did not influence the phosphorylation or expression level of STAT6 in IL-4–treated macrophages (Figure S9I). These data indicate that IL-4–induced oligomeric NPM1 recruits KDM5b to form an epigenetic complex at *Tsc1* promoter and mediates the erasing of H3K4me3 modification, thereby suppressing *Tsc1* gene transcription.

Loss of Function of NPM1 Improves Tissue Repair and Cardiac Function After MI

The in vivo therapeutic benefit of targeting NPM1 for MI was then explored. The in vivo administration of NPM1 inhibitor NSC348884 in MI model mice improved cardiac function with the increased ejection fraction and fractional shortening, whereas it had no effect on cardiac function in mice with sham operation (Figure S10A through S10C). Moreover, NSC348884 ameliorated adverse cardiac remodeling with the decreased left ventricular volume, left ventricular internal diameter, and left ventricular posterior wall after MI (Figure S10D). The fibrosis area in heart tissue after MI was also attenuated in mice given NSC348884 (Figure S10E). Consistent with the results in Npm1-cKO mice, the levels of various genes indicative of the reparative macrophage phenotype, cardiac repair, and angiogenesis were significantly increased, whereas the expression of fibrotic genes was markedly reduced in the cardiac tissue of mice given NSC348884 (Figure S10F and S10G).

ASO, a short strand of deoxyribonucleotide analogue, has been found to recruit ribonuclease H to cleave the target mRNA and inhibit mRNA translation.[44] ASO was in vivo applied to treat MI-induced cardiac fibrosis.[45] Two types of ASOs, ASO1 and ASO2, with modifications specifically targeting NPM1 both could markedly decrease mRNA and protein levels of NPM1 in macrophages (Figure 8A, Figure S11A). The mRNA and protein expression levels of TSC1 and reparative phenotype genes such as *Arg1* and *Mrc1* were significantly upregulated in IL-4–activated BMDMs after transfection with either type of ASO (Figure 8A and 8B). The in vivo administration of ASO1 had notably beneficial effects on MI-induced cardiac dysfunction, as reflected by the increased ejection fraction and fractional shortening (Figure 8C through 8E), and the ameliorated indicators of adverse cardiac remodeling, including left ventricular volume, left ventricular internal diameter, interventricular septum, and

ORIGINAL RESEARCH ARTICLE

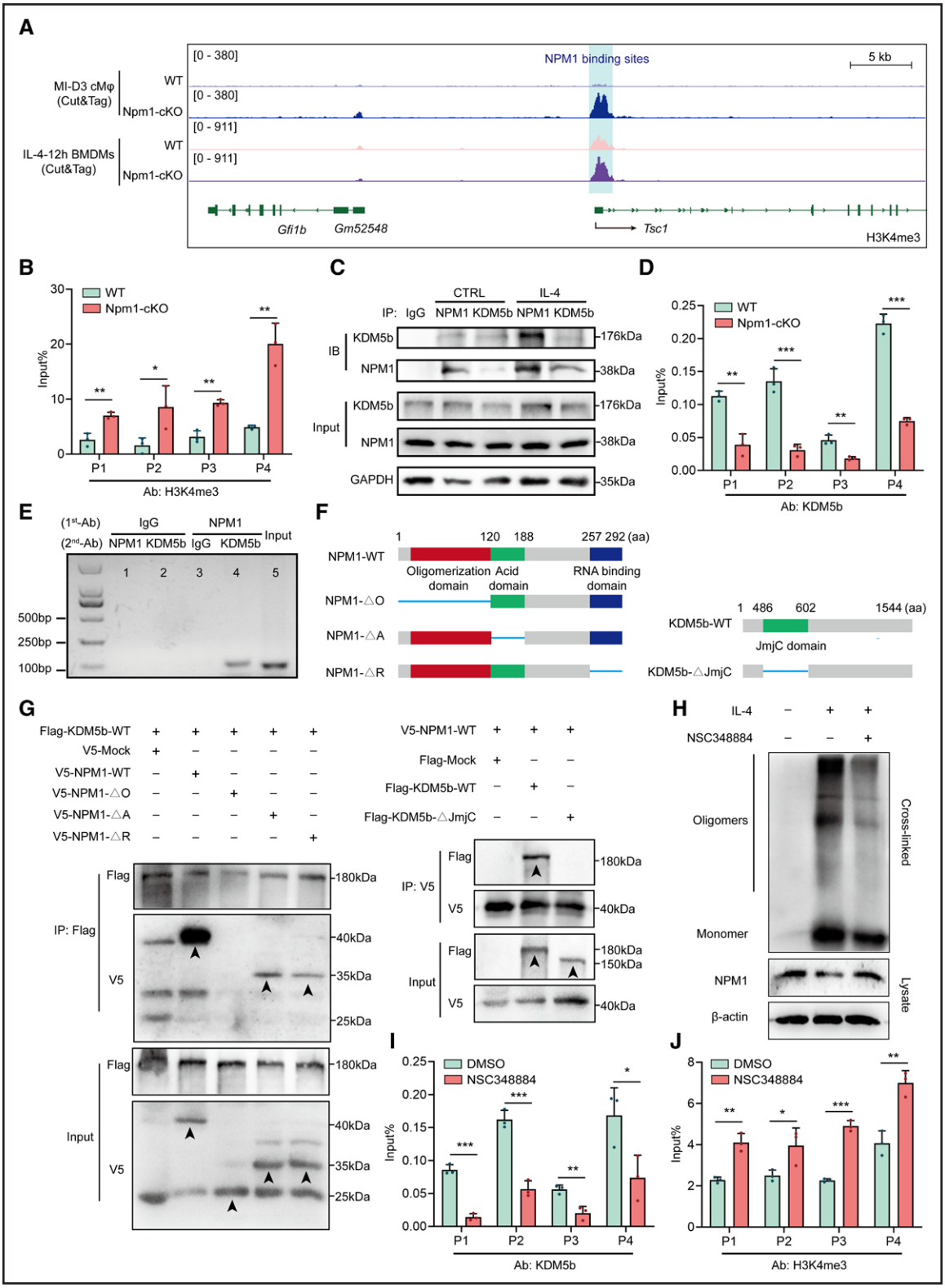

Figure 7. Oligomeric NPM1 inhibits TSC1 expression through recruitment of KDM5b to reduce H3K4me3 modification level of *Tsc1* promoter.

A, Integrative Genomics Viewer analysis of H3K4me3 signal in the gene locus of *Tsc1*. Cut&Tag assays for H3K4me3 levels were performed in cardiac macrophages at day 3 after MI and BMDMs treated with IL-4 for 12 hours from WT and Npm1-cKO mice. **B**, ChIP-qPCR analysis of H3K4me3 levels at the promoter of *Tsc1* in Npm1-cKO and WT BMDMs with IL-4 stimulation (n=3 per group; Student *t* test). **C**, Immunoblot analysis of NPM1 and KDM5b in protein complexes immunoprecipitated with anti-NPM1 or anti-KDM5b antibody from lysates of WT BMDMs with or without IL-4 stimulation. **D**, ChIP-qPCR analysis of KDM5b enrichment at *Tsc1* promoter in Npm1-cKO and WT BMDMs with IL-4 stimulation (n=3 per group; Student *t* test). **E**, Re-ChIP-PCR assay of KDM5B-NPM1 interaction at the *Tsc1* promoter in BMDMs (*Continued*)

Figure 7 Continued. stimulated with IL-4 for 24 hours. First-round ChIP (first antibody) was performed with anti-NPM1 antibody or IgG. Eluted samples were subjected to second-round ChIP (second antibody). Line 5 was the input. **F,** Schematic diagram of V5-tagged WT NPM1 plasmid and mutants with deletion of the oligomerization domain (Δ O), the acid domain (Δ A), or the RNA binding domain (Δ R). Schematic diagram of Flag-tagged WT KDM5b plasmid and mutant with deletion of the JmjC domain (Δ JmjC). **G**, HEK293T cells were cotransfected with the Flag-tagged WT KDM5b (Flag-KDM5b-WT), V5-tagged WT NPM1 (V5-NPM1-WT), or the indicated mutants followed by immunoprecipitation with anti-Flag antibody (**left**) or anti-V5 antibody (**right**) and immunoblot analysis with anti-V5 antibody or anti-Flag antibody. **H**, Immunoblot analysis of NPM1 oligomerization in BMDMs treated with IL-4 alone or a combination of IL-4 and NSC348884. **I** and **J**, ChIP-qPCR analysis of KDM5b enrichment (**I**) or H3K4me3 modification (**J**) at *Tsc1* promoter in IL-4–stimulated WT BMDMs treated with DMSO or NSC348884 (n=3 per group; Student *t* test). **P*<0.05; ***P*<0.01; ****P*<0.001. Ab indicates antibody; BMDM, bone marrow–derived macrophage; ChIP-qPCR, chromatin immunoprecipitation followed by quantitative polymerase chain reaction; CTRL, control; DMSO, dimethyl sulfoxide; IB, immunoblot; IgG, immunoglobulin; IL-4, interleukin 4; IP, immunoprecipitation; MI, myocardial infarction; NPM1, nucleophosmin 1; TSC1, TSC complex subunit 1; and WT, wild type.

left ventricular posterior wall (Figure S11B and S11C). A remarkable reduction in fibrosis area was also found in the heart tissue of mice given ASO1 after MI (Figure 8F). In addition, ASO1 administration significantly upregulated the expression levels of genes indicative of the reparative phenotype, cardiac repair, and angiogenesis function, while inhibiting the expression of fibrotic genes in cardiac tissue after infarction (Figure 8G and 8H). A noticeably increased capillary density and reduced myofibroblast amount were consistently observed in cardiac tissue of mice given ASO1 after MI (Figure 8I). These results demonstrate that the in vivo loss of function of NPM1 mediated by specific inhibitor and ASO administration can improve cardiac dysfunction and alleviate adverse cardiac remodeling after MI by boosting the tissue repair capacity of cardiac macrophages.

In summary, our finding provides evidence that NPM1 recruits histone demethylase KDM5b to *Tsc1* promoter for erasing H3K4me3 modification on ischemic stress, then inhibits TSC1 expression and enhances mTOR signaling activation, which blunts cardiac repair mediated by macrophages (Figure S12). Loss of function of NPM1 might be one potential way to ameliorate cardiac ischemic injury and promote tissue repair after heart attack.

DISCUSSION

Cardiac macrophages are indispensable to modulate local immune responses in heart tissue after MI. The transition of cardiac macrophages to reparative phenotype determines the resolution of inflammatory responses and efficient tissue repair postinfarction.[46] Although genetic mutation of NPM1 has been implicated in the pathogenesis of acute myeloid leukemia and certain solid tumors, its involvement in cardiovascular diseases is not well established.[15] A previous study found that NPM1 promoted atherosclerosis by inducing vascular inflammation and endothelial dysfunction through the NF-κB (nuclear factor-κB) signaling pathway.[47] Our study identifies the key role of NPM1 in controlling an inflammatory phenotype of cardiac macrophages to antagonize cardiac repair after MI. Macrophage-specific deletion of NPM1 could promote cardiac tissue repair and ameliorate cardiac dysfunction and adverse remodeling after MI. The inhibited mTOR pathway mediated by the upregulated TSC1 shifted cardiac macrophages toward OXPHOS metabolism under NPM1 deficiency, which facilitated the reparative phenotype during ischemic tissue repair. This study provides evidence that the epigenetic machinery mediated by interaction between NPM1 and KDM5b orchestrates cardiac macrophage phenotypic transition and postinfarction tissue repair through metabolic reprogramming.

Increased evidence has revealed the importance of the reparative subpopulation of cardiac macrophages in postinfarct wound healing.[46] The phenotypes of cardiac macrophages largely determine their functional characteristics. At first, our findings exhibited that macrophage-specific deletion of NPM1 considerably amplified the reparative subpopulation of cardiac macrophages in ischemic heart tissues, as measured by widely acknowledged markers of reparative macrophages: Arg1^{+}, Ly6C^{low} and CD206^{+}.[48,49] Nevertheless, function maturation of cardiac-repair macrophages also relies on the expression of effector molecules.[50] For instance, MerTK is essential for cardiac macrophages to conduct their repair effect,[51] and MFGE8 coordinates with MerTK to favor VEGFA secretion and local healing after infarction.[26] Moreover, the secreted angiogenic growth factors GDF15 and CNPY2 facilitate cell proliferation and tissue repair after MI.[51] Tmsb4x provides cardiomyocytes with a permissive environment for regeneration and improves blood supply to ischemic lesions.[28] On the basis of these previous findings, our study demonstrates that the macrophage-specific knockout or pharmacological inhibition of NPM1 markedly increases the expression of a wide range of reparative molecules, including MerTK, MFGE8, GDF15, CNPY2, and Tmsb4x, in cardiac macrophages to facilitate cardiac repair. These functional molecules may protect cardiomyocytes from ischemia and inflammation-induced apoptosis and enhance their survival by generating a favorable environment with improved blood supply and reduced harmful factors. These reparative molecules simultaneously limit excessive fibrosis and adverse remodeling. These findings highlight a potential therapeutic strategy for enhancing cardiac recovery through facilitating reparative macrophages mediated by NPM1 inhibition.

Forceful OXPHOS is capable of driving proinflammatory macrophages to adopt a reparative phenotype.[52] Our

ORIGINAL RESEARCH ARTICLE

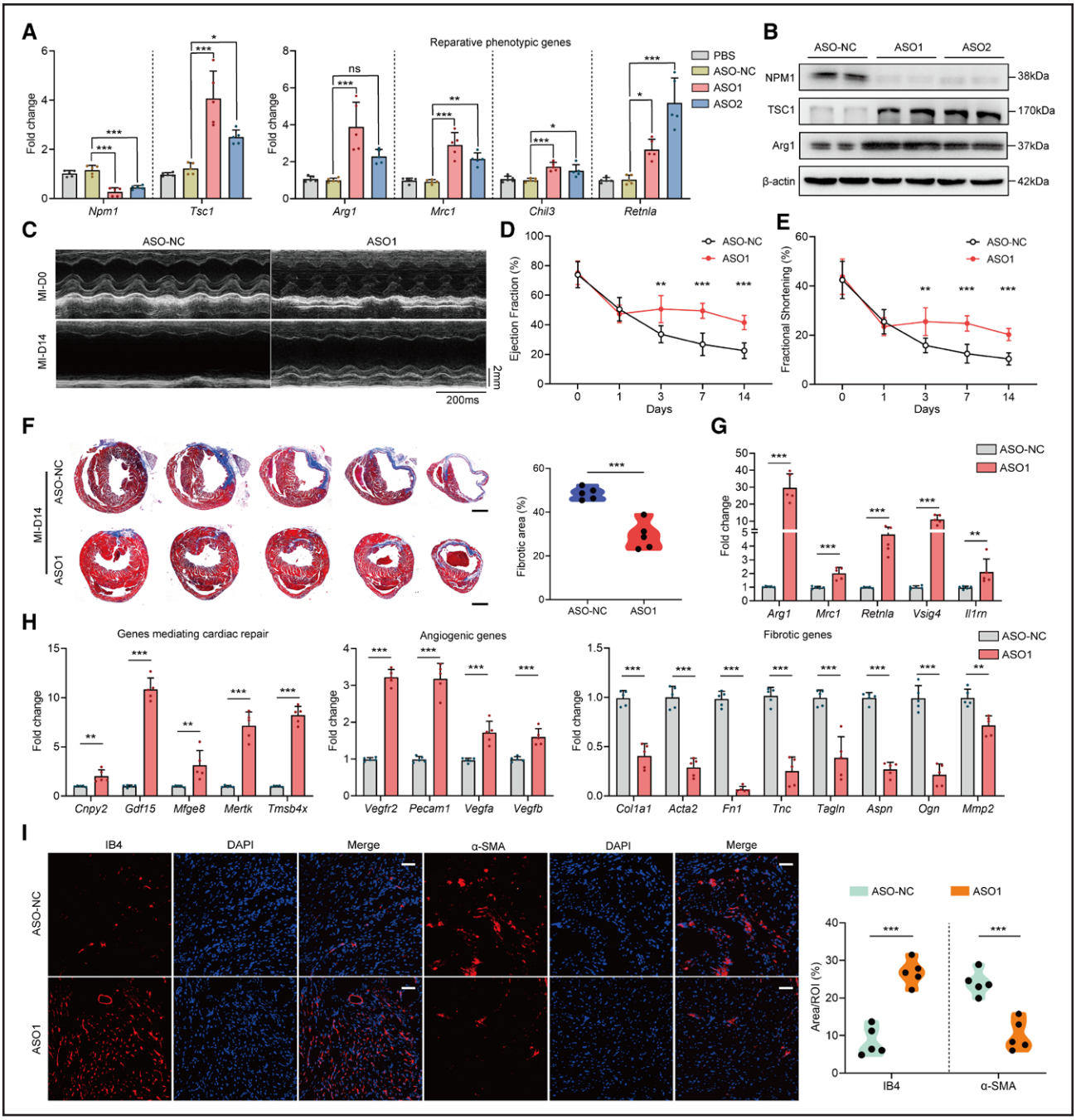

Figure 8. ASO targeting NPM1 improves tissue repair and cardiac function after MI.

A, The mRNA expression levels of *Npm1*, *Tsc1*, and genes indicative of reparative phenotype in WT bone marrow–derived macrophages without transfection (PBS) or transfected with ASO control (ASO-NC), ASO1, or ASO2, and then stimulated with IL-4 for 24 hours (n=5 per group; ANOVA followed by Bonferroni test). **B**, Immunoblot analysis of NPM1, TSC1, and Arg1 protein levels in WT bone marrow–derived macrophages transfected with ASO-NC, ASO1, or ASO2 followed by stimulation with IL-4 for 24 hours. **C**, Representative echocardiograms obtained from WT mice given ASO-NC or ASO1 at day 0 and day 14 after MI. **D** and **E**, Echocardiographic measurements of left ventricular ejection fraction (**D**) and fractional shortening (**E**) of WT mice given ASO-NC or ASO1 as in **C** at the indicated day after MI (n=8 per group; 2-way ANOVA followed by Bonferroni test). **F**, Masson trichrome staining of heart sections from WT mice given ASO-NC or ASO1 at day 14 after MI and quantification of fibrotic area (n=5 per group; unpaired Student *t* test). Scale bar=1 mm. **G**, The mRNA expression levels of genes indicative of reparative macrophage phenotype in ischemic cardiac tissues of WT mice given ASO-NC or ASO1 at day 5 after MI (n=5 per group; unpaired Student *t* test). **H**, The mRNA expression levels of genes mediating cardiac repair, angiogenesis, and fibrosis in ischemic cardiac tissues of WT mice given ASO-NC or ASO1 at day 5 (for cardiac repair–related genes) or 14 (for angiogenic and fibrotic genes) after MI (n=5 per group; unpaired Student *t* test). **I**, Immunofluorescence staining of IB4 and α-SMA expression in the border zone of heart tissues from WT mice given ASO-NC or ASO1 at day 14 after MI. Scale bar=50 μm (n=5 per group; unpaired Student *t* test). **P*<0.05; ***P*<0.01; ****P*<0.001. ASO indicates antisense oligonucleotide; DAPI, 4′,6-diamidino-2-phenylindole; IB4, isolectin-B4; MI, myocardial infarction; NPM1, nucleophosmin 1; PBS, phosphate buffered saline; ROI, region of interest; α-SMA, α-smooth muscle actin; TSC1, TSC complex subunit 1; and WT, wild type.

experiments demonstrate that NPM1 deletion coordinates cellular OXPHOS metabolism of cardiac macrophages and the conversion to reparative phenotype. The metabolic profiling results indicate that NPM1 deficiency leads to reduced amounts of citrate and succinate, 2 remarkable inducible metabolites during the HIF-1α–mediated Warburg effect. This metabolic adaptation to aerobic glycolysis contributes to the NF-κB–dependent inflammatory cytokine production and M1-like effector shift in macrophages.[53] Furthermore, NPM1 deficiency facilitates the introduction of pyruvic acid into the TCA cycle, as evidenced by the reduction of lactic acid and the elevation of other TCA intermediates. Unlike proinflammatory macrophages, NPM1-deficient macrophages increase the conversion of isocitrate to α-ketoglutaric acid, indicating intensified glutamine catabolism and macrophage alternative activation.[54] Nonetheless, our findings outline a novel landscape of intermediate metabolite alteration in the TCA cycle during the reparative phenotypic transition of cardiac macrophages, which was previously controlled by NPM1. In sum, NPM1 disturbs macrophage alternative activation through impeding oxidative mitochondrial respiration and rewiring metabolic patterns.

Previous studies have established a link between epigenetic modifications and cellular metabolism mediated by the mTORC1 (rapamycin complex 1) signaling pathway.[55] Recent evidence implies that TSC1, a critical negative regulator of the mTOR complex, modulates bioenergetic metabolism by orchestrating the mTOR signaling cascades.[56] Here, we discover that NPM1 directly binds to *Tsc1* promoter and inhibits its transcription and expression. NPM1 acts as an epigenetic factor to target *Tsc1* gene and recruit histone demethylase KDM5b, forming an inhibitory epigenetic complex and erasing H3K4me3 level at *Tsc1* promoter, finally inhibiting reparative transition through the mTOR pathway. Although IL-4–induced phosphorylated STAT6 has been reported to enhance the expression of most reparative phenotypic markers, including Arg1, it turns out that the NPM1/TSC1 pathway and STAT6 mediate the effects of IL-4 independently.[57] Our results indicate an alternative epigenetic mechanism by which IL-4 regulates the macrophage phenotype. In addition, some observations suggest that oligomer formation of NPM1 is essential for its biological functions, particularly its histone chaperone activity.[43] Our results consistently validate that the oligomerization domain of NPM1 is necessary to the interaction with KDM5b and its biological function in impairing cardiac repair. Overall, this work provides insight into the interplay between epigenetic regulation and metabolic programming. By controlling the transcription of TSC1 and orchestrating metabolic status, NPM1 functions as a "molecular switch" in macrophage phenotype transition through repressing OXPHOS remodeling to compromise postinfarction cardiac repair.

Last but not least, our investigation provides a potential therapeutic strategy with ASOs targeting NPM1 for improving cardiac dysfunction and alleviating adverse cardiac remodeling after MI. ASOs, which bind and cleave target RNAs, are capable of impeding protein expression without genetic modification.[58] ASOs have gained attraction due to their reduced susceptibility to nuclease degradation, prolonged plasma stability, and higher cell-uptake affinity compared with small interfering RNAs.[59] Although ASOs have been widely used in clinical trials, only a handful of ASOs have been authorized for cardiovascular diseases, and they are scarcely used for treating ischemic heart disease.[60] Our study provides evidence that ASOs targeting NPM1 are effective in promoting cardiac functional recovery by boosting the tissue repair capacity of cardiac macrophages, implying that specific ASOs hold promise as a clinical immunomodulation treatment for ischemic heart diseases.

In summary, our study uncovers the key role of NPM1 in antagonizing tissue repair and preservation of cardiac function after MI through the crosstalk between epigenetic regulation and metabolic programming and highlights novel pathogenic mechanisms in ischemic tissue injury and cardiac maladaptive remodeling, which presents a promising target for the treatment of ischemic heart attack.

Limitations of This Study

There are several limitations that should be considered in this study. First, although the *Lyz2-cre* strain is highly efficient in manipulating macrophages, it is not a very specific marker for them. The genetic deletion may potentially affect the population of neutrophils and dendritic cells. For enhanced specificity, usage of *F4/80-cre* can be considered in future research. Second, although this study demonstrates the cardioprotective effects of the functional loss of NPM1 in the MI model, it should be acknowledged that the animal model is inevitably limited in its ability to fully replicate the complex pathological status of MI in patients. Third, although the study discovers the reprogramming of metabolic status in macrophages mainly mediated by the mTOR pathway, it remains unclear how this pathway specifically alters the activity of certain enzymes. Finally, our results highlight the therapeutic effect of NPM1-targeted ASOs and the inhibitor NSC348884. However, optimal dosing and long-term effects need to be fully explored. Further investigation involving MI models of large animals and primates is therefore necessary to fully evaluate the efficacy and safety of these potential drugs.

ARTICLE INFORMATION

Received May 8, 2023; accepted February 2, 2024.

Affiliations

Shanghai Institute of Transplantation, Renji Hospital, Shanghai Jiao Tong University School of Medicine, Shanghai, China (Z.Z., B.W.). Key Laboratory of Arrhythmias of the Ministry of Education of China, Shanghai East Hospital, Tongji University School of Medicine, Shanghai, China (S.Z., X.D., Z.Z.). Naval Medical Center, Naval Medical University, Shanghai, China (Y.Z.).

Acknowledgments

Drs S. Zhang and Y. Zhang, X. Duan, and Dr B. Wang performed the experiments, analyzed the data, and interpreted the results. Drs S. Zhang and Y. Zhang designed the experiments and drafted the manuscript. Dr Z. Zhan conceived the idea, designed the experiments, analyzed the data, revised the manuscript, and provided funding for this study. The authors thank Figdraw (www.figdraw.com) for help drawing the figures.

Sources of Funding

This work was supported by the National Key R&D Program of China (2019YFA0801502 and 2023YFC2307003), and the National Natural Science Foundation of China (82070415 and 82371825).

Disclosures

None.

Supplemental Material

Expanded Methods

Figures S1–S12

Tables S1–S3

Supplemental References 61–64

Uncropped Gel Blots

REFERENCES

1. Cai S, Zhao M, Zhou B, Yoshii A, Bugg D, Villet O, Sahu A, Olson GS, Davis J, Tian R. Mitochondrial dysfunction in macrophages promotes inflammation and suppresses repair after myocardial infarction. *J Clin Invest*. 2023;133:e159498. doi: 10.1172/JCI159498
2. Marinković G, Koenis DS, de Camp L, Jablonowski R, Graber N, de Waard V, de Vries CJ, Goncalves I, Nilsson J, Jovinge S, et al. S100a9 links inflammation and repair in myocardial infarction. *Circ Res*. 2020;127:664–676. doi: 10.1161/CIRCRESAHA.120.315865
3. Nahrendorf M, Pittet MJ, Swirski FK. Monocytes: protagonists of infarct inflammation and repair after myocardial infarction. *Circulation*. 2010;121:2437–2445. doi: 10.1161/CIRCULATIONAHA.109.916346
4. Cao DJ, Schiattarella GG, Villalobos E, Jiang N, May HI, Li T, Chen ZJ, Gillette TG, Hill JA. Cytosolic DNA sensing promotes macrophage transformation and governs myocardial ischemic injury. *Circulation*. 2018;137:2613–2634. doi: 10.1161/CIRCULATIONAHA.117.031046
5. Phan AT, Goldrath AW, Glass CK. Metabolic and epigenetic coordination of T cell and macrophage immunity. *Immunity*. 2017;46:714–729. doi: 10.1016/j.immuni.2017.04.016
6. Pålsson-McDermott EM, O'Neill LAJ. Targeting immunometabolism as an anti-inflammatory strategy. *Cell Res*. 2020;30:300–314. doi: 10.1038/s41422-020-0291-z
7. Mounier R, Théret M, Arnold L, Cuvellier S, Bultot L, Göransson O, Sanz N, Ferry A, Sakamoto K, Foretz M, et al. AMPKα1 regulates macrophage skewing at the time of resolution of inflammation during skeletal muscle regeneration. *Cell Metab*. 2013;18:251–264. doi: 10.1016/j.cmet.2013.06.017
8. Palmieri EM, Menga A, Martín-Pérez R, Quinto A, Riera-Domingo C, De Tullio G, Hooper DC, Lamers WH, Ghesquière B, McVicar DW, et al. Pharmacologic or genetic targeting of glutamine synthetase skews macrophages toward an M1-like phenotype and inhibits tumor metastasis. *Cell Rep*. 2017;20:1654–1666. doi: 10.1016/j.celrep.2017.07.054
9. Ventham NT, Kennedy NA, Nimmo ER, Satsangi J. Beyond gene discovery in inflammatory bowel disease: the emerging role of epigenetics. *Gastroenterology*. 2013;145:293–308. doi: 10.1053/j.gastro.2013.05.050
10. Dong C, Yuan T, Wu Y, Wang Y, Fan TW, Miriyala S, Lin Y, Yao J, Shi J, Kang T, et al. Loss of FBP1 by Snail-mediated repression provides metabolic advantages in basal-like breast cancer. *Cancer Cell*. 2013;23:316–331. doi: 10.1016/j.ccr.2013.01.022
11. Tang Y, Feng M, Su Y, Ma T, Zhang H, Wu H, Wang X, Shi S, Zhang Y, Xu Y, et al. Jmjd4 facilitates Pkm2 degradation in cardiomyocytes and is protective against dilated cardiomyopathy. *Circulation*. 2023;147:1684–1704. doi: 10.1161/CIRCULATIONAHA.123.064121
12. Zhou F, Müller-Tidow C. NPM1 functions in epitranscriptomics. *Nat Genet*. 2019;51:1436–1437. doi: 10.1038/s41588-019-0510-z
13. Grisendi S, Bernardi R, Rossi M, Cheng K, Khandker L, Manova K, Pandolfi PP. Role of nucleophosmin in embryonic development and tumorigenesis. *Nature*. 2005;437:147–153. doi: 10.1038/nature03915
14. Zhang H, Chen Q, Zhang Q, Gan H, Li H, Chen S, Shan H, Pang P, He H. DDX24 mutation alters NPM1 phase behavior and disrupts nucleolar homeostasis in vascular malformations. *Int J Biol Sci*. 2023;19:4123–4138. doi: 10.7150/ijbs.84097
15. Karimi Dermani F, Gholamzadeh Khoei S, Afshar S, Amini R. The potential role of nucleophosmin (NPM1) in the development of cancer. *J Cell Physiol*. 2021;236:7832–7852. doi: 10.1002/jcp.30406
16. Thygesen K, Alpert JS, Jaffe AS, Chaitman BR, Bax JJ, Morrow DA, White HD; Executive Group on behalf of the Joint European Society of Cardiology (ESC)/American College of Cardiology (ACC)/American Heart Association (AHA)/World Heart Federation (WHF) Task Force for the Universal Definition of Myocardial Infarction. Fourth universal definition of myocardial infarction (2018). *J Am Coll Cardiol*. 2018;72:2231–2264. doi: 10.1016/j.jacc.2018.08.1038
17. Edgar L, Akbar N, Braithwaite AT, Krausgruber T, Gallart-Ayala H, Bailey J, Corbin AL, Khoyratty TE, Chai JT, Alkhalil M, et al. Hyperglycemia induces trained immunity in macrophages and their precursors and promotes atherosclerosis. *Circulation*. 2021;144:961–982. doi: 10.1161/CIRCULATIONAHA.120.046464
18. Benjamini Y, Krieger AM, Yekutieli D. Adaptive linear step-up procedures that control the false discovery rate. *Biometrika*. 2006;93:491–507. doi: 10.1093/biomet/93.3.491
19. Vanhaverbeke M, Vausort M, Veltman D, Zhang L, Wu M, Laenen G, Gillijns H, Moreau Y, Bartunek J, Van De Werf F, et al; EU-CardioRNA COST Action CA17129. Peripheral blood RNA levels of *QSOX1* and *PLBD1* are new independent predictors of left ventricular dysfunction after acute myocardial infarction. *Circ Genom Precis Med*. 2019;12:e002656. doi: 10.1161/CIRCGEN.119.002656
20. Liu Y, Morley M, Brandimarto J, Hannenhalli S, Hu Y, Ashley EA, Tang WH, Moravec CS, Margulies KB, Cappola TP, et al; MAGNet consortium. RNA-seq identifies novel myocardial gene expression signatures of heart failure. *Genomics*. 2015;105:83–89. doi: 10.1016/j.ygeno.2014.12.002
21. Witt E, Hammer E, Dörr M, Weitmann K, Beug D, Lehnert K, Nauck M, Völker U, Felix SB, Ameling S. Correlation of gene expression and clinical parameters identifies a set of genes reflecting LV systolic dysfunction and morphological alterations. *Physiol Genomics*. 2019;51:356–367. doi: 10.1152/physiolgenomics.00111.2018
22. Smythies JA, Sun M, Masson N, Salama R, Simpson PD, Murray E, Neumann V, Cockman ME, Choudhry H, Ratcliffe PJ, et al. Inherent DNA-binding specificities of the HIF-1α and HIF-2α transcription factors in chromatin. *EMBO Rep*. 2019;20:e46401. doi: 10.15252/embr.201846401
23. Welsh P, Preiss D, Hayward C, Shah ASV, McAllister D, Briggs A, Boachie C, McConnachie A, Padmanabhan S, Welsh C, et al. Cardiac troponin T and troponin I in the general population. *Circulation*. 2019;139:2754–2764. doi: 10.1161/CIRCULATIONAHA.118.038529
24. Ammirati E, Cannistraci CV, Cristell NA, Vecchio V, Palini AG, Tornvall P, Paganoni AM, Miendlarzewska EA, Sangalli LM, Monello A, et al. Identification and predictive value of interleukin-6^{+} interleukin-10^{+} and interleukin-6^{-} interleukin-10^{+} cytokine patterns in ST-elevation acute myocardial infarction. *Circ Res*. 2012;111:1336–1348. doi: 10.1161/CIRCRESAHA.111.262477
25. Kempf T, Zarbock A, Widera C, Butz S, Stadtmann A, Rossaint J, Bolomini-Vittori M, Korf-Klingebiel M, Napp LC, Hansen B, et al. GDF-15 is an inhibitor of leukocyte integrin activation required for survival after myocardial infarction in mice. *Nat Med*. 2011;17:581–588. doi: 10.1038/nm.2354
26. Howangyin KY, Zlatanova I, Pinto C, Ngkelo A, Cochain C, Rouanet M, Vilar J, Lemitre M, Stockmann C, Fleischmann BK, et al. Myeloid-epithelial-reproductive receptor tyrosine kinase and milk fat globule epidermal growth factor 8 coordinately improve remodeling after myocardial infarction via local delivery of vascular endothelial growth factor. *Circulation*. 2016;133:826–839. doi: 10.1161/CIRCULATIONAHA.115.020857
27. Yin W, Guo J, Zhang C, Alibhai FJ, Li SH, Billia P, Wu J, Yau TM, Weisel RD, Li RK. Knockout of canopy 2 activates p16^{Ink4a} pathway to impair cardiac repair. *J Mol Cell Cardiol*. 2019;132:36–48. doi: 10.1016/j.yjmcc.2019.04.018
28. Gladka MM, Kohela A, Molenaar B, Versteeg D, Kooijman L, Monshouwer-Kloots J, Kremer V, Vos HR, Huibers MMH, Haigh JJ, et al. Cardiomyocytes stimulate angiogenesis after ischemic injury in a ZEB2-dependent manner. *Nat Commun*. 2021;12:84. doi: 10.1038/s41467-020-20361-3
29. Palla AR, Ravichandran M, Wang YX, Alexandrova L, Yang AV, Kraft P, Holbrook CA, Schürch CM, Ho ATV, Blau HM. Inhibition of prostaglandin-degrading enzyme 15-PDGH rejuvenates aged muscle mass and strength. *Science*. 2021;371:eabc8059. doi: 10.1126/science.abc8059
30. Barallobre-Barreiro J, Radovits T, Fava M, Mayr U, Lin WY, Ermolaeva E, Martínez-López D, Lindberg EL, Duregotti E, Daróczi L, et al. Extracellular matrix in heart failure: role of ADAMTS5 in proteoglycan remodeling. *Circulation*. 2021;144:2021–2034. doi: 10.1161/CIRCULATIONAHA.121.055732

31. Geissler A, Ryzhov S, Sawyer DB. Neuregulins: protective and reparative growth factors in multiple forms of cardiovascular disease. *Clin Sci (Lond)*. 2020;134:2623–2643. doi: 10.1042/CS20200230
32. Matsushima S, Sadoshima J. The role of sirtuins in cardiac disease. *Am J Physiol Heart Circ Physiol*. 2015;309:H1375–H1389. doi: 10.1152/ajpheart.00053.2015
33. Ikeuchi M, Matsusaka H, Kang D, Matsushima S, Ide T, Kubota T, Fujiwara T, Hamasaki N, Takeshita A, Sunagawa K, et al. Overexpression of mitochondrial transcription factor a ameliorates mitochondrial deficiencies and cardiac failure after myocardial infarction. *Circulation*. 2005;112:683–690. doi: 10.1161/CIRCULATIONAHA.104.524835
34. Nachmani D, Bothmer AH, Grisendi S, Mele A, Bothmer D, Lee JD, Monteleone E, Cheng K, Zhang Y, Bester AC, et al. Germline NPM1 mutations lead to altered rRNA 2′-O-methylation and cause dyskeratosis congenita. *Nat Genet*. 2019;51:1518–1529. doi: 10.1038/s41588-019-0502-z
35. Inoki K, Kim J, Guan KL. AMPK and mTOR in cellular energy homeostasis and drug targets. *Annu Rev Pharmacol Toxicol*. 2012;52:381–400. doi: 10.1146/annurev-pharmtox-010611-134537
36. Zhu L, Yang T, Li L, Sun L, Hou Y, Hu X, Zhang L, Tian H, Zhao Q, Peng J, et al. TSC1 controls macrophage polarization to prevent inflammatory disease. *Nat Commun*. 2014;5:4696. doi: 10.1038/ncomms5696
37. Daniel B, Nagy G, Horvath A, Czimmerer Z, Cuaranta-Monroy I, Poliska S, Hays TT, Sauer S, Francois-Deleuze J, Nagy L. The IL-4/STAT6/PPARγ signaling axis is driving the expansion of the RXR heterodimer cistrome, providing complex ligand responsiveness in macrophages. *Nucleic Acids Res*. 2018;46:4425–4439. doi: 10.1093/nar/gky157
38. Soldi M, Mari T, Nicosia L, Musiani D, Sigismondo G, Cuomo A, Pavesi G, Bonaldi T. Chromatin proteomics reveals novel combinatorial histone modification signatures that mark distinct subpopulations of macrophage enhancers. *Nucleic Acids Res*. 2017;45:12195–12213. doi: 10.1093/nar/gkx821
39. Goode DK, Obier N, Vijayabaskar MS, Lie ALM, Lilly AJ, Hannah R, Lichtinger M, Batta K, Florkowska M, Patel R, et al. Dynamic gene regulatory networks drive hematopoietic specification and differentiation. *Dev Cell*. 2016;36:572–587. doi: 10.1016/j.devcel.2016.01.024
40. Nicodeme E, Jeffrey KL, Schaefer U, Beinke S, Dewell S, Chung CW, Chandwani R, Marazzi I, Wilson P, Coste H, et al. Suppression of inflammation by a synthetic histone mimic. *Nature*. 2010;468:1119–1123. doi: 10.1038/nature09589
41. Wang H, Fan Z, Shliaha PV, Miele M, Hendrickson RC, Jiang X, Helin K. H3K4me3 regulates RNA polymerase II promoter-proximal pause-release. *Nature*. 2023;615:339–348. doi: 10.1038/s41586-023-05780-8
42. He R, Kidder BL. H3K4 demethylase KDM5b regulates global dynamics of transcription elongation and alternative splicing in embryonic stem cells. *Nucleic Acids Res*. 2017;45:6427–6441. doi: 10.1093/nar/gkx251
43. Balusu R, Fiskus W, Rao R, Chong DG, Nalluri S, Mudunuru U, Ma H, Chen L, Venkannagari S, Ha K, et al. Targeting levels or oligomerization of nucleophosmin 1 induces differentiation and loss of survival of human AML cells with mutant NPM1. *Blood*. 2011;118:3096–3106. doi: 10.1182/blood-2010-09-309674
44. Liang XH, Nichols JG, Sun H, Crooke ST. Translation can affect the antisense activity of RNase H1-dependent oligonucleotides targeting mRNAs. *Nucleic Acids Res*. 2018;46:293–313. doi: 10.1093/nar/gkx1174
45. Micheletti R, Plaisance I, Abraham BJ, Sarre A, Ting CC, Alexanian M, Maric D, Maison D, Nemir M, Young RA, et al. The long noncoding RNA *Wisper* controls cardiac fibrosis and remodeling. *Sci Transl Med*. 2017;9:eaai9118. doi: 10.1126/scitranslmed.aai9118
46. Shirakawa K, Endo J, Kataoka M, Katsumata Y, Yoshida N, Yamamoto T, Isobe S, Moriyama H, Goto S, Kitakata H, et al. IL (interleukin)-10-STAT3-Galectin-3 axis is essential for osteopontin-producing reparative macrophage polarization after myocardial infarction. *Circulation*. 2018;138:2021–2035. doi: 10.1161/CIRCULATIONAHA.118.035047
47. Rao C, Liu B, Huang D, Chen R, Huang K, Li F, Dong N. Nucleophosmin contributes to vascular inflammation and endothelial dysfunction in atherosclerosis progression. *J Thorac Cardiovasc Surg*. 2021;161:e377–e393. doi: 10.1016/j.jtcvs.2019.10.152
48. Huang CK, Dai D, Xie H, Zhu Z, Hu J, Su M, Liu M, Lu L, Shen W, Ning G, et al. Lgr4 governs a pro-inflammatory program in macrophages to antagonize post-infarction cardiac repair. *Circ Res*. 2020;127:953–973. doi: 10.1161/CIRCRESAHA.119.315807
49. Shin NS, Marlier A, Xu L, Doilicho N, Linberg D, Guo J, Cantley LG. Arginase-1 is required for macrophage-mediated renal tubule regeneration. *J Am Soc Nephrol*. 2022;33:1077–1086. doi: 10.1681/ASN.2021121548
50. Matrone G, Xia B, Chen K, Denvir MA, Baker AH, Cooke JP. Fli1^{+} cells transcriptional analysis reveals an Lmo2-Prdm16 axis in angiogenesis. *Proc Natl Acad Sci USA*. 2021;118:e2008559118. doi: 10.1073/pnas.2008559118
51. Guo J, Zhang Y, Mihic A, Li SH, Sun Z, Shao Z, Wu J, Weisel RD, Li RK. A secreted protein (Canopy 2, CNPY2) enhances angiogenesis and promotes smooth muscle cell migration and proliferation. *Cardiovasc Res*. 2015;105:383–393. doi: 10.1093/cvr/cvv010
52. Mouton AJ, Li X, Hall ME, Hall JE. Obesity, hypertension, and cardiac dysfunction: novel roles of immunometabolism in macrophage activation and inflammation. *Circ Res*. 2020;126:789–806. doi: 10.1161/CIRCRESAHA.119.312321
53. Jha AK, Huang SC, Sergushichev A, Lampropoulou V, Ivanova Y, Loginicheva E, Chmielewski K, Stewart KM, Ashall J, Everts B, et al. Network integration of parallel metabolic and transcriptional data reveals metabolic modules that regulate macrophage polarization. *Immunity*. 2015;42:419–430. doi: 10.1016/j.immuni.2015.02.005
54. Liu PS, Wang H, Li X, Chao T, Teav T, Christen S, Di Conza G, Cheng WC, Chou CH, Vavakova M, et al. α-ketoglutarate orchestrates macrophage activation through metabolic and epigenetic reprogramming. *Nat Immunol*. 2017;18:985–994. doi: 10.1038/ni.3796
55. Su X, Yu Y, Zhong Y, Giannopoulou EG, Hu X, Liu H, Cross JR, Rätsch G, Rice CM, Ivashkiv LB. Interferon-γ regulates cellular metabolism and mRNA translation to potentiate macrophage activation. *Nat Immunol*. 2015;16:838–849. doi: 10.1038/ni.3205
56. Byles V, Covarrubias AJ, Ben-Sahra I, Lamming DW, Sabatini DM, Manning BD, Horng T. The TSC-mTOR pathway regulates macrophage polarization. *Nat Commun*. 2013;4:2834. doi: 10.1038/ncomms3834
57. Wang F, Zhang S, Vuckovic I, Jeon R, Lerman A, Folmes CD, Dzeja PP, Herrmann J. Glycolytic stimulation is not a requirement for M2 macrophage differentiation. *Cell Metab*. 2018;28:463–475.e4. doi: 10.1016/j.cmet.2018.08.012
58. Crooke ST, Witztum JL, Bennett CF, Baker BF. RNA-targeted therapeutics. *Cell Metab*. 2018;27:714–739. doi: 10.1016/j.cmet.2018.03.004
59. Liang XH, Sun H, Hsu CW, Nichols JG, Vickers TA, De Hoyos CL, Crooke ST. Golgi-endosome transport mediated by M6PR facilitates release of antisense oligonucleotides from endosomes. *Nucleic Acids Res*. 2020;48:1372–1391. doi: 10.1093/nar/gkz1171
60. Witztum JL, Gaudet D, Freedman SD, Alexander VJ, Digenio A, Williams KR, Yang Q, Hughes SG, Geary RS, Arca M, et al. Volanesorsen and triglyceride levels in familial chylomicronemia syndrome. *N Engl J Med*. 2019;381:531–542. doi: 10.1056/NEJMoa1715944
61. DeBerge M, Yeap XY, Dehn S, Zhang S, Grigoryeva L, Misener S, Procissi D, Zhou X, Lee DC, Muller WA, et al. MerTK cleavage on resident cardiac macrophages compromises repair after myocardial ischemia reperfusion injury. *Circ Res*. 2017;121:930–940. doi: 10.1161/CIRCRESAHA.117.311327
62. Zhang Y, Gao Y, Jiang Y, Ding Y, Chen H, Xiang Y, Zhan Z, Liu X. Histone demethylase KDM5b licenses macrophage-mediated inflammatory responses by repressing Nfkbia transcription. *Cell Death Differ*. 2023;30:1279–1292. doi: 10.1038/s41418-023-01136-x
63. Baker N, Wade S, Triolo M, Girgis J, Chwastek D, Larrigan S, Feige P, Fujita R, Crist C, Rudnicki MA, et al. The mitochondrial protein OPA1 regulates the quiescent state of adult muscle stem cells. *Cell Stem Cell*. 2022;29:1315–1332.e9. doi: 10.1016/j.stem.2022.07.010
64. Wu Y, Zhou L, Liu H, Duan R, Zhou H, Zhang F, He X, Lu D, Xiong K, Xiong M, et al. LRP6 downregulation promotes cardiomyocyte proliferation and heart regeneration. *Cell Res*. 2021;31:450–462. doi: 10.1038/s41422-020-00411-7